Space Science Reviews (2024) 220:13
https://doi.org/10.1007/s11214-024-01044-7

# Strong Gravitational Lensing and Microlensing of Supernovae

**Sherry H. Suyu[1,2,3] · Ariel Goobar[4] · Thomas Collett[5] · Anupreeta More[6,7] · Giorgos Vernardos[8]**

Received: 2 June 2023 / Accepted: 30 December 2023 / Published online: 5 February 2024


**Abstract**
Strong gravitational lensing and microlensing of supernovae (SNe) are emerging as a new probe of cosmology and astrophysics in recent years. We provide an overview of this nascent research field, starting with a summary of the first discoveries of strongly lensed SNe. We describe the use of the time delays between multiple SN images as a way to measure cosmological distances and thus constrain cosmological parameters, particularly the Hubble constant, whose value is currently under heated debates. New methods for measuring the time delays in lensed SNe have been developed, and the sample of lensed SNe from the upcoming Rubin Observatory Legacy Survey of Space and Time (LSST) is expected to provide competitive cosmological constraints. Lensed SNe are also powerful astrophysical probes. We review the usage of lensed SNe to constrain SN progenitors, acquire high-z SN spectra through lensing magnifications, infer SN sizes via microlensing, and measure properties of dust in galaxies. The current challenge in the field is the rarity and difficulty in finding lensed SNe. We describe various methods and ongoing efforts to find these spectacular explosions, forecast the properties of the expected sample of lensed SNe from upcoming surveys particularly the LSST, and summarize the observational follow-up requirements to enable the various scientific studies. We anticipate the upcoming years to be exciting with a boom in lensed SN discoveries.

**Keywords** Gravitational lensing: strong · Gravitational lensing: micro · Supernovae: general · (Cosmology:) distance scale · (Cosmology:) cosmological parameters · (ISM:) dust, extinction

## 1 Brief History

In an insightful and pioneering publication, Refsdal (1964) pointed out that supernovae (SNe) would be particularly interesting sources for studies involving strong gravitational lensing. This was arguably among the biggest early milestones in the field of gravitational lensing, following the realisation by Zwicky (1937) that the scenario, first proposed by Einstein in 1936, had realistic applications in extra-galactic astronomy. Refsdal pointed out that the measurement of the time delay between the arrival of SN images could be used to infer the Hubble constant ($H_0$).

Extended author information available on the last page of the article

### 1.1 History of Searches for Lensed SNe Behind Clusters

The idea to use "gravitational telescopes", i.e., known lensing galaxy clusters, to boost the faint signals from distant supernovae started to get traction about thirty years ago (Kovner and Paczynski 1988; Sullivan et al. 2000; Gunnarsson and Goobar 2003). Since the lensing magnification boosts the signal from the faint distant source behind the lens by a factor of $\mu$, but leaves the dominant foreground sky noise unaffected, the signal-to-noise ratio scales as $SNR \propto \mu\sqrt{t}$ (where $t$ is the exposure time), hence leading to a gain factor $\mu^2$ in exposure length. However, the solid angle at the source planes shrinks by a factor $\mu$ behind the lens. Thus, the net gain/loss of searching for supernovae behind massive clusters is therefore a non-trivial combination of field of view, limiting depth, and supernova luminosity functions. Although not spectroscopically confirmed, several SN candidates were eventually found in cadenced observations in the Near-IR at the Very Large Telescopes (VLT) of the European Southern Observatory (ESO) (Stanishev et al. 2009; Goobar et al. 2009), including a $z = 1.7$ core-collapse SN behind Abell 1689, with a lens model inferred magnification $\mu = 4.3 \pm 0.3$ (Amanullah et al. 2011). In spite of the limitations of the survey, Petrushevska et al. (2016) demonstrated the power of gravitational lensing to place meaningful limits on the rate of core-collapse supernovae at very high redshifts.

### 1.2 Discoveries!

PS1-10afx was first reported by Chornock et al. (2013) as an unusual superluminous SN. However, shortly thereafter, Quimby et al. (2013) showed that it was a perfect match to a lensed SN Ia at redshift $z = 1.388$, with a large amplification, $\mu \sim 30$. Quimby et al. (2014) eventually also identified a foreground lens, at $z = 1.117$. Even if the putative lensing object was too close to the SN, it was consistent with lensing models and existing data. Since the lensed SN Ia classification only gained acceptance four years after the explosion, further investigation of the lensing nature of the SN or its type was not possible. Moreover, a subsequent single-band HST imaging (PI: Chornock) proved insufficient to verify the presence of any lensed images of the SN host galaxy.

The first detection of multiple images from a supernova came with SN Refsdal at redshift $z = 1.49$ (Kelly et al. 2015), found in Hubble Space Telescope (HST) surveys of the massive lensing galaxy cluster MACS J1149.6+2223 at $z = 0.54$. Based on both light curve shapes and spectroscopy, SN Refsdal was classified as a Type II SN, resembling the iconic SN 1987A in the LMC (Kelly et al. 2016b). This is a peculiar class of faint SNe, quite rare in the local universe. At the time of discovery, 4 multiple images of the SN were visible with HST (images S1-S4, see Fig. 1 taken from Grillo et al. 2018), in a cross configuration around one of the foreground cluster galaxies. There are two other images of the background spiral galaxy hosting the SN, labelled as SX (inset (a) in Fig. 1) and SY (the northern-most image, just outside the top-right corner of inset (a)).

Using mass models of the cluster, the discovery team (Kelly et al. 2015) predicted that SY happened before S1-S4, whereas SX would appear after S1-S4. However, the time of SX reappearance was uncertain from their model, ranging from 1 to 10 years. To refine the delay prediction, Grillo et al. (2016) used the Multi Unit Spectroscopic Explorer (MUSE; Bacon et al. 2010) on ESO's VLT to obtain spectroscopic observations of the field. The spectroscopic redshift measurements helped to separate foreground lenses from background sources. This spectroscopic data set was shared with multiple modelling teams, who attempted to predict the reappearance of image SX using the new observational data. Teams predicted their delays before the reappearance (Treu et al. 2016; Jauzac et al. 2016; Grillo

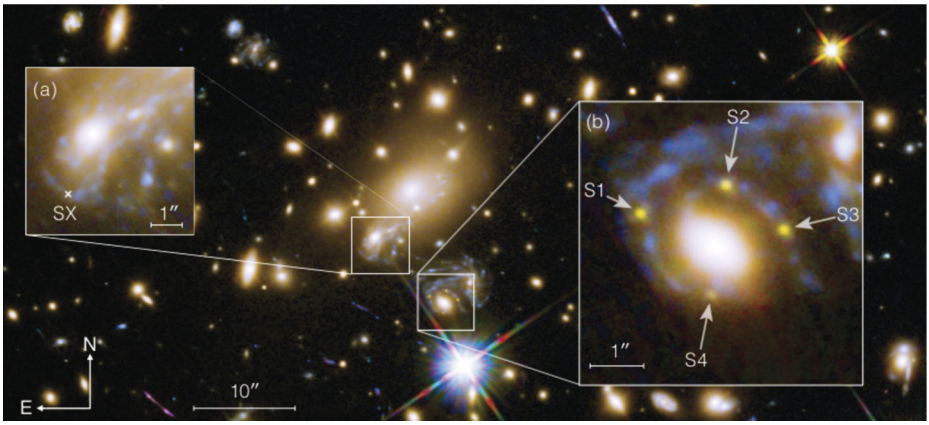


**Fig. 1** Hubble Space Telescope image of SN Refsdal, the first strongly lensed SN system with spatially resolved images. Inset (a) shows the image SX that was detected in December 2015 (Kelly et al. 2016a), and inset (b) shows the multiple images S1, S2, S3 and S4 that were first discovered in November 2014 (Kelly et al. 2015). There is another image SY located in the northern most image of the spiral host galaxy, next to the top-right corner of the inset (a). Image taken from Grillo et al. (2018). Original image credit: NASA, ESA/Hubble

et al. 2016; Kawamata et al. 2016), providing a true blind test of the predictions and the modelling capabilities. Most teams predicted a short time delay of SX with respect to S1, within a year's time. Kelly et al. (2016a) detected the reappearance of SX in December 2015, and the resulting constraint on the time delay and magnification of SX agreed well with the predictions from two teams (Grillo et al. 2016; Kawamata et al. 2016).

Through the monitoring of the multiple images of SN Refsdal, Rodney et al. (2016) have measured the time delays and magnification ratios among images S1, S2, S3 and S4. The time-delay measurement for image SX from subsequent monitoring is $376.0^{+5.6}_{-5.5}$ days relative to image S1 (Kelly et al. 2023b). This time-delay measurement with a relative uncertainty of 1.5% provides the first opportunity for a precise $H_0$ measurement from lensed SNe, which we describe more in Sect. 2.3.

The first spatially resolved multiply-imaged Type Ia supernova, iPTF16geu, was detected by the intermediate Palomar Transient Factory (Goobar et al. 2017). As shown in Fig. 2, the ground-based imager at iPTF could not spatially resolve the very compact system with Einstein radius $\theta_{\rm E} = 0.3''$. However, because of the "standard candle" nature of SNe Ia, it became clear that strong lensing was the most likely explanation, since the SN was more than 30 standard deviations brighter than the expectations for a SN Ia at its measured redshift, $z = 0.409$. The spectra used to classify the supernova showed spectral lines from both the host galaxy at the same redshift, but also the deflecting galaxy at $z = 0.216$. Thanks to multi-band follow-up with HST, an accurate (model independent) measurement of the magnification was made, $\mu = 67.8^{+2.6}_{-2.9}$ (Dhawan et al. 2020), after correction for non-negligible extinction by dust in both the host and lens galaxies. The time delays between the SN images for this system were very small, about a day or less (More et al. 2017; Dhawan et al. 2020). The flux ratios between the supernova images (see Fig. 2) were not consistent with expectations from lensing, hinting contributions from stellar microlensing (More et al. 2017). This was further confirmed after differential dust extinction from within the lensing galaxy was also accounted for (Mörtsell et al. 2020).

In 2021, another strongly lensed SN, SN Requiem, was discovered in archival HST imaging of the galaxy cluster MACSJ0138.0−2155 by Rodney et al. (2021). A bright quiescent

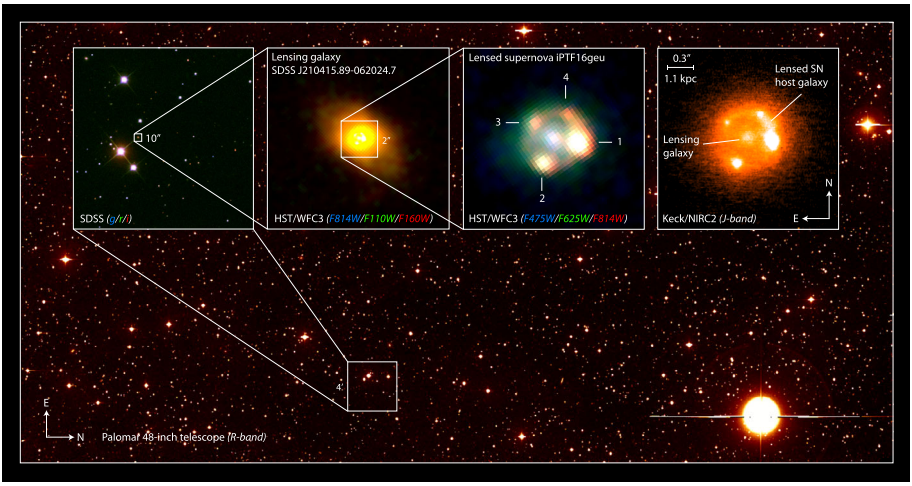


**Fig. 2** Wide-field image from iPTF showing the portion of the CCD camera where iPTF16geu was found in modest seeing ($2''$). The insets show how the strong lensing nature, a quadruple lens with an Einstein radius of only $0.3''$, could be verified using HST imaging in the optical, and laser-guide-star adaptive-optics imaging from Keck in the Near-IR. Image credit: J. Johansson

and evolved elliptical galaxy at redshift $z = 1.95$ is lensed into giant arcs by the galaxy cluster as shown in Fig. 3, making this system one of the brightest NIR objects (e.g., Newman et al. 2018). Near the giant arcs are three point sources that were present in the single-epoch image in 2016 (Newman et al. 2018), but absent in the 2019 HST image (HST Program - REQUIEM; HST-GO-15663; PI:Akhshik). These 3 point sources are identified as multiple images of a SN hosted in the $z = 1.95$ galaxy, and the SN is likely to be of Type Ia. Based on the differences in the colour of the 3 SN images and SN Ia templates, the time delays could be estimated from the single-epoch observation in 2016, although with large uncertainties. The predicted time delays suggest that the fourth image of SN Requiem will appear in the future (circa 2037).

Recently, Goobar et al. (2023) discovered another strongly lensed SNe Ia, named Supernova Zwicky (a.k.a. SN 2022qmx), in the Zwicky Transient Facility (ZTF; Bellm et al. 2019). The discovery of this system is similar to the case of iPTF16geu – the multiple lensed SN Ia images are closely separated (with an Einstein radius of $\theta_{\rm E} \sim 0.17''$) and not spatially resolved by ZTF, thus resulting in a brightness through lensing magnification that is substantially higher than expected for a SN Ia. Pierel et al. (2023) obtained HST imaging of this system, showing clearly the four multiple images of the SN Ia in a symmetric configuration. Based on the single-epoch photometry of the SN Ia images, Pierel et al. (2023) measured short time delays of $< 1$ day between the multiple images, which are consistent with the predictions from their multiple lens mass models obtained using different lensing software. Both Goobar et al. (2023) and Pierel et al. (2023) find anomalous flux ratios of the SN images compared to the smooth mass model predictions, indicating the presence of dust, millilensing and/or microlensing.

The fifth system of spatially-resolved lensed SN is reported very recently by Chen et al. (2022). A SN was lensed by one of the galaxies in the galaxy cluster Abell 370 in 2010 into three multiple images, and Chen et al. (2022) discovered it in archival HST image, similar to the way that SN Resfdal was found. Based on their cluster lens mass modeling,

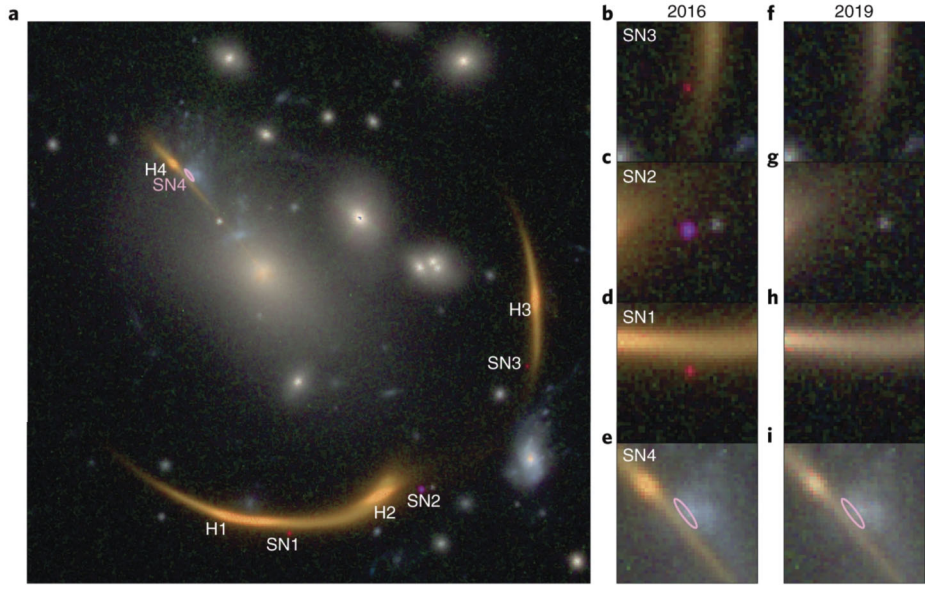


**Fig. 3** Panel a): Color image of SN Requiem showing arc-like images of the distant host galaxy (H1-H4), the three SN images (SN1-SN3) and an ellipse pointing out the expected location of SN4. Panels b-i): zoomed-in regions around the SN locations from the data taken in 2016 (b-e) and 2019 (f-i). Figure taken from Rodney et al. (2021)

Chen et al. (2022) estimated the rest-frame age of the SN for each of the three SN images, with the youngest one being a mere $\sim 6$ hours after explosion. Using the early-phase light curve obtained in the single-epoch HST observations with multiple filters, Chen et al. (2022) classified the SN as a core-collapse SN and measured its pre-explosion radius of $\sim 500 R_{\odot}$, consistent with a red supergiant. The estimated photometric redshift of the SN host galaxy is $\sim 3$.

The sixth system is the first strongly lensed SN detected with the James Webb Space Telescope (JWST) in the imaging of the galaxy cluster PLCK-G165.7+67.0, named SN H0pe (Frye et al. 2023; Polletta et al. 2023). This strong lensing cluster was discovered through the detection and follow-up of the brightest, strongly lensed dusty star-forming galaxies on the sky from Planck and Herschel (Cañameras et al. 2015; Planck Collaboration et al. 2015). This cluster and a lensed dusty galaxy have been observed and studied by Cañameras et al. (2015), Harrington et al. (2016), Cañameras et al. (2018), Frye et al. (2019), Pascale et al. (2022) prior to the JWST observations. Upon the discovery of SN H0pe (occurring in a background elliptical galaxy that is strongly lensed into a prominent arc), Frye et al. (2023) obtained additional JWST imaging and spectroscopy of the system in order to constrain the time delays of the SN images through photometry (Pierel et al., submitted) and spectroscopy (Chen et al., in prep.). Several papers are forthcoming to use this system to study SN Ia, SN host galaxy, dusty star-forming galaxy and cosmology (e.g., Johansson et al., Caminha et al., Kamieneski et al., Pascale et al., in prep.).

These first few strongly lensed SNe have opened a new window to probe cosmology and supernovae through these spectacular phenomena. Two reviews (Oguri 2019; Liao et al. 2022) on gravitationally lensed transients have illustrated the exciting utilities of lensed transients. Compared to these two reviews, we focus and dive deeper into the specific case of

strongly lensed supernovae. In Sect. 2, we review the potential of lensed SNe as a cosmological probe. In Sect. 3, we describe the use of lensed SNe as an astrophysical probe, such as constraining the SN progenitors and dust in galaxies. In Sect. 4, we present various searches of lensed SNe and the expected rates in current and upcoming surveys. We summarise in Sect. 5.

## 2 Cosmological Probe

While the idea of using lensed SNe for measuring the Hubble constant dates back to Refsdal (1964), this time-delay method was first realised with lensed quasars that were discovered decades before lensed SNe, starting with the first lensed quasar system found by Walsh et al. (1979). The use of lensed quasars as a cosmological probe is reviewed by Birrer et al. (2024) in this collection (see also, e.g., Treu and Marshall 2016; Suyu et al. 2018; Treu et al. 2022). We briefly summarise the approach of time-delay cosmography in Sect. 2.1, and focus on SNe as lensed background sources, which are "standardisable candles" and a relative distance indicator. In Sect. 2.2, we describe approaches to measure time delays of lensed SNe, particularly novel ones through spectroscopic observations of SNe, which complement conventional techniques using photometric light curves. In Sect. 2.3, we show the present cosmological constraints and future forecasts from lensed SNe.

### 2.1 Jackpot: Two Cosmological Probes in One

We describe the various distance measurements that we can obtain from strongly lensed SNe, through the lensing time delays and the SN light curves. We briefly summarise the determination of the lensing distances that are covered in detail in the parallel reviews by, e.g., Birrer et al. (2024), and focus particularly on the new aspects that SNe bring.

The expression for the time delay between images $i$ and $j$ of a lensed SN is

$$\Delta t_{ij} = \frac{D_{\Delta t}}{c} \Delta \tau_{ij}, \tag{1}$$

where $D_{\Delta t}$ is the time-delay distance, $c$ is the speed of light, and $\tau$ is the Fermat potential. The time-delay distance (e.g., Refsdal 1964; Suyu et al. 2010) is defined by

$$D_{\Delta t} \equiv (1 + z_{\rm d}) \frac{D_{\rm d} D_{\rm s}}{D_{\rm ds}}, \tag{2}$$

where $z_{\rm d}$ is the deflector (lens) redshift, and $D_{\rm d}$, $D_{\rm s}$, and $D_{\rm ds}$ are the angular diameter distance to the deflector, to the source, and between the deflector and the source, respectively. The Fermat potential difference between two SN image positions $\boldsymbol{\theta}_i$ and $\boldsymbol{\theta}_j$ (with corresponding source position $\boldsymbol{\beta}$) is

$$\Delta \tau_{ij} = \tau(\boldsymbol{\theta}_i; \boldsymbol{\beta}) - \tau(\boldsymbol{\theta}_j; \boldsymbol{\beta}), \tag{3}$$

where the Fermat potential is

$$\tau(\boldsymbol{\theta}; \boldsymbol{\beta}) = \frac{1}{2}(\boldsymbol{\theta} - \boldsymbol{\beta})^2 - \psi(\boldsymbol{\theta}), \tag{4}$$

and $\psi(\boldsymbol{\theta})$ is the lens potential. The dimensionless surface mass density $\kappa(\boldsymbol{\theta})$, a.k.a. lensing convergence, is related to the lens potential via the Poisson equation,

$$2\kappa(\boldsymbol{\theta}) = \nabla^2\psi(\boldsymbol{\theta}) \tag{5}$$

From Eq. (1), we see that by measuring the time delays $\Delta t_{ij}$ and modelling the deflection and line-of-sight mass distributions to get $\Delta\tau_{ij}$, we can infer the time-delay distance $D_{\Delta t}$. Since $D_{\Delta t}$ is a combination of three angular diameter distances (Eq. (2)) and is thus proportional to $H_0^{-1}$, time-delay lenses allow us to measure directly $H_0$ with weak dependence on other cosmological parameters.

When the lens galaxy stellar velocity dispersion is measured, then the combination of time delays, velocity dispersion and high-resolution imaging of the lens system allows $D_{\rm d}$ to be measured (e.g., Paraficz and Hjorth 2009; Jee et al. 2015, 2019), in addition to $D_{\Delta t}$. The joint constraint of $D_{\Delta t}$ and $D_{\rm d}$ provides even more leverage on determining cosmological parameters (e.g., Jee et al. 2016; Yıldırım et al. 2020).

It is clear from Eq. (4) that in order to constrain $H_0$ with strong lens time delays, one needs to know both the 2D lens potential and the unlensed source position, neither of which are directly observable. The use of lens modelling is required to infer these quantities. However, strong lens models are subject to degeneracies, which are a major source of uncertainty for time-delay cosmography (Schneider and Sluse 2014). The largest problem is the mass-sheet degeneracy: re-scaling any model of the lensing convergence $\kappa$ and adding a constant sheet of surface mass density leaves the predicted images unchanged, but alters the predicted time delay between the images (Falco et al. 1985). Breaking the mass-sheet degeneracy is therefore necessary to constrain $H_0$ from any lens with observations of image positions and time delays. In order to break the mass-sheet degeneracy, additional information is required, either non-lensing information (e.g., the dynamical mass of the system), the presence of sources at multiple redshifts (though see Schneider 2014) or knowledge of the intrinsic luminosity or size of the unlensed source (Kolatt and Bartelmann 1998). It is on this final point – a known luminosity of the source – that strongly lensed SNe shine as a powerful potential cosmological probe.

In this context, Type Ia SNe play a special role. Thanks to the homogeneity of their luminosity, these thermonuclear explosions could be used as sharp distance estimators to measure the accelerated expansion of the universe (Riess et al. 1998; Perlmutter et al. 1999), leading to the discovery of dark energy. State-of-the-art SN Ia cosmological surveys have demonstrated that the intrinsic luminosity of SNe Ia only varies by about 0.1 mag (Betoule et al. 2014; Scolnic et al. 2018). Birrer et al. (2022) have shown the great benefit of these sharp distance indicators to break the mass-sheet degeneracy to improve the accuracy of the measurements of the Hubble constant from time delays.

Despite the great opportunity presented by having a lensed standard candle, the exploitation of lensed SNe poses an additional challenge: microlensing by stars (Dobler and Keeton 2006). The intrinsic size of a SN is comparable to the Einstein radius of an individual star in the lens galaxy, a case analogous to microlensing of lensed quasars (Vernardos et al. 2023, in prep.). This means that observed magnification is sensitive to the – essentially unobservable – positions of stars in the lensing galaxy. Worse, as the supernova expands, the SN atmosphere crosses microlensing caustics. This causes a change in total magnification of the supernova and differential magnification across the atmosphere (Bagherpour et al. 2006; Goldstein et al. 2018; Huber et al. 2019; Mörtsell et al. 2020); this means that the light curves of each image can look quite different even though they are formed from the same background source, as illustrated in Fig. 4. This makes it a challenge for measuring accurate

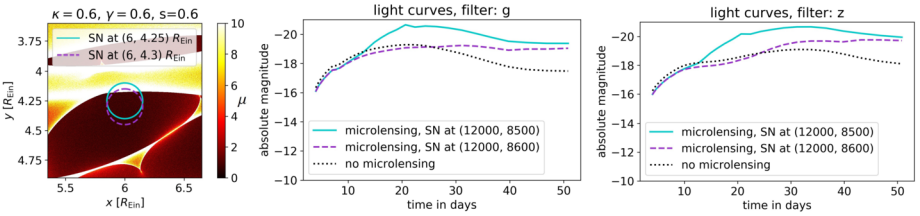


**Fig. 4** Examples of Type Ia SNe light curves with significant microlensing. Left panel: a map of microlensing magnifications ($\mu$, indicated by the color bar) on the source plane as a result from stars in the foreground lens galaxy. The map is for a lensed SN image with convergence $\kappa = 0.6$, shear $\gamma = 0.6$, and smooth dark matter fraction $s = 0.6$. In this example, the Einstein radius for the mean microlens is $R_{\rm Ein} = 7.2 \times 10^{-3}$ pc. The two circles in solid cyan and dashed magenta indicate the size of a SN Ia at 21 rest-frame days after explosion. Middle and right panels: microlensed light curves in the g-band (middle panel) and z-band (right panel) corresponding to the SN positions shown in the left panel (solid cyan and dashed magenta). The intrinsic light curve without microlensing is shown in dotted black. When the expanding photosphere of the SN crosses a microlensing caustic with high $\mu$, its light curve changes substantially relative to the no-microlensing case. Figure taken from Huber et al. (2019)

time delays between images, though early colour curves can overcome this due to an achromatic phase in the microlensing at early times (Goldstein et al. 2018; Huber et al. 2021b) as can spectroscopic observations of absorption lines in the SN atmosphere (Johansson et al. 2021; Bayer et al. 2021).

The SNe never reach a large enough size for the microlensing effect of multiple stars to average out, so microlensing makes it hard to standardise lensed SNe. The scale of this problem depends in detail on the magnification of the image, the type of the image (time-delay minimum, maximum or saddle) and fraction of density in stars at the location of the image (e.g., Schechter and Wambsganss 2002; Huber et al. 2021b). For high macro-magnification images, the scatter can be as large as 1 magnitude in flux (Schechter and Wambsganss 2002; Yahalomi et al. 2017; Diego et al. 2022), entirely washing out the possibility of using lensed SNe as a standard candle. For images forming further from the Einstein Radius, and particularly for large mass systems where the dark matter fraction is higher at the Einstein radius, the scatter is much smaller and can be less than the intrinsic scatter of a Type Ia SN.

Foxley-Marrable et al. (2018) found that 20 percent of lensed SNe will contain an image with scatter comparable to the intrinsic scatter of a Type Ia supernova luminosity, assuming the dark matter fractions of elliptical galaxies derived in Auger et al. (2010) and a Saltpeter IMF. However, these standardisable images only form far beyond the Einstein radius of the lens. This means that the counter images are very close to the centre of the lens and demagnified. Measuring time delays will therefore be challenging, although the faint images arrive second so follow-up with a larger telescope may ameliorate this problem.

The 20 percent standardisable fraction is subject to two key caveats: the stellar initial mass function is assumed to be Salpeter-like and the ellipticity of the lensing mass follows that of the light. The assumption of a particular IMF sets the stellar-to-dark matter fraction. Figure 5 shows the importance of this assumption: at very high stellar fraction there are no strongly lensed images with minimal microlensing scatter (Weisenbach et al. 2021). With a population of lensed SNe, Foxley-Marrable et al. (2018) found that observing the amount of microlensing induced scatter can be used to constrain the IMF of the lens galaxy, with strong sensitivity for lenses with Einstein radius between 0.2″ and 0.5″. The assumption that mass follows light produces more elliptical lens mass distributions than is seen in cold-dark-matter-only simulations. Increasing the ellipticity of the lens moves the dashed lines in Fig. 5 to the left. Strongly lensed images can form at lower magnification, where microlensing

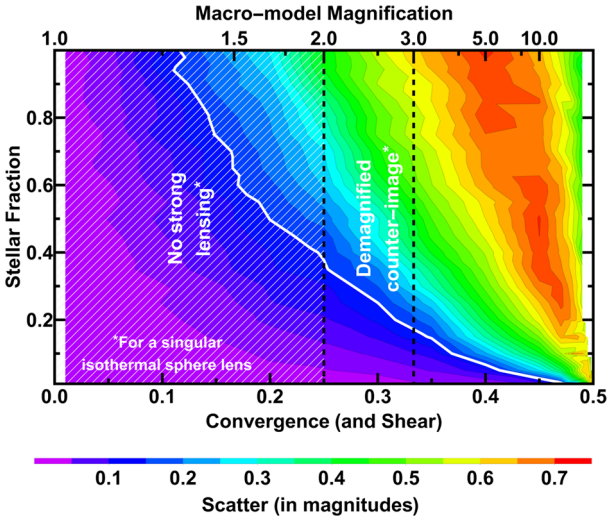


**Fig. 5** Microlensing induced scatter (indicated by the color bar) for a point source lensed by a Singular Isothermal Sphere (SIS) macromodel as a function of stellar fraction and macro-magnification. For an SIS, the convergence and shear magnitude (shown in the $x$-axis) are the same at any given location on the lens plane. Scatter is lower for the lensed SN image that is far from the Einstein radius (with lower convergence/shear), but there is a limit since a convergence below 0.25 produces only single images (i.e., no strong lensing) and convergence below $\sim$0.35 produces a faint counterimage (close to lens center) that makes time-delay measurements more challenging. Image credit: Luke Weisenbach, modified based on Weisenbach et al. (2021)

is less significant. If real lenses are more spherical, then the standardisable fraction will fall. Therefore, the standardisation of lensed supernovae is subject to somewhat uncertain astrophysics. Exactly what we observe from a large sample of lensed supernovae will inform not just cosmology but also the astrophysics of matter in the strong lensing galaxy.

Despite microlensing distortions on the light curves of SNe and reductions in the number of standardisable SN, lensed SNe still have various advantages over the more conventional lensed quasars for time-delay cosmography. The drastically varying brightness of lensed SNe enable shorter monitoring campaigns (months) to obtain the light curves and thus more efficient measurements of time delays. Simulations of microlensed SN light curves with realistic photometric uncertainties showed that time delays can still be recovered accurately and precisely (Huber et al. 2019; Pierel and Rodney 2019), and the dominant source of uncertainty in the time delays is typically photometric uncertainties rather than microlensing distortions (Huber et al. 2021a). Another advantage of lensed SNe is that SNe fade after several months, revealing both the lens galaxy and the lensed SN host galaxy more clearly that enable more accurate lens mass modelling (e.g., Ding et al. 2021). In particular, spatially-resolved stellar kinematics of the foreground lens galaxy can be more readily acquired after the SN images fade, and the combination of lensing and kinematic data allows one to break the mass-sheet degeneracy (e.g., Barnabè et al. 2012; Yıldırım et al. 2020, 2023; Birrer et al. 2020; Shajib et al. 2023). Stellar kinematic maps of the lensed SN host galaxy would further constrain the lens mass distribution (Chirivì et al. 2020). We therefore anticipate lensed SNe to be an efficient cosmological probe in the upcoming era of time-domain astronomy when hundreds of such lensed SN events are expected to happen (e.g., Oguri and Marshall 2010; Quimby et al. 2014; Goldstein et al. 2019; Wojtak et al. 2019).

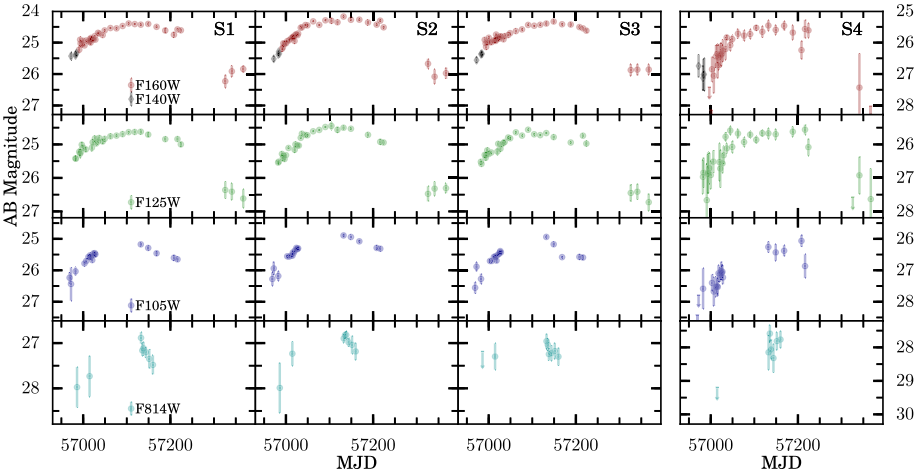


**Fig. 6** Light curves of SN Refsdal from Hubble Space Telescope imaging in multiple wavelength filters. Each row consists of the light curves obtained in the specific filter that is indicated in the leftmost panel. Each column shows one of the four SN images, S1-S4 (left to right), that are indicated on the top panels. Each panel shows the observed AB magnitude as a function of the observer-frame days. Figure taken from Rodney et al. (2016)

## 2.2 Time-Delay Measurements

The time delays between multiple lensed images are a key ingredient for time-delay cosmography. The fractional uncertainties in the time delays translate directly to the fractional uncertainties in the $D_{\Delta t}$ and $D_{\rm d}$ measurements (Eq. (1)).

Traditionally, the measurements of time delays involve monitoring the lens system to acquire the light curves of either lensed quasars (e.g., Fassnacht et al. 2002; Courbin et al. 2018; Millon et al. 2020a,b) or lensed supernovae (e.g., Rodney et al. 2016; Dhawan et al. 2020). Figure 6 shows an example of the light curves of the four images (S1, S2, S3 and S4) of SN Refsdal obtained by Rodney et al. (2016). Curve-shifting techniques that account for microlensing distortions are then applied to these light curves to extract the time delays (e.g., Tewes et al. 2013; Pierel and Rodney 2019; Millon et al. 2020c). By making use of the characteristic SN Ia SEDs, Dhawan et al. (2020) used SN Ia template light curves to fit to the HST images of iPTF16geu and measured the 3 independent time delays between the four SN images. New machine learning approaches such as random forests are also being developed to infer the delays of microlensed SN Ia systems from the light curves (e.g., Huber et al. 2021a).

SNe are not only drastically changing their brightness, but their spectra also evolve substantially. The spectroscopic evolution of supernovae offers a new avenue to measure the time delays that are complementary and competitive to the light-curve techniques, as demonstrated by Johansson et al. (2021) for the case of iPTF16geu. For the most common type of core-collapse supernovae, SNe IIP, where the light curves rise fast to peak and then reach a plateau phase that could last for hundreds of days, spectral time delays may be the best way forward as there is a tight correlation between the velocity and time (e.g., $v(t) \propto t^{-0.464\pm0.017}$; Nugent et al. 2006). Figure 7 shows an example of the spectra of Type IIP SN1999em from the TARDIS simulation (Kerzendorf and Sim 2014; Vogl et al. 2019, 2020) at multiple epochs after explosion (Bayer et al. 2021). These epochs (in rest-frame days) are in the

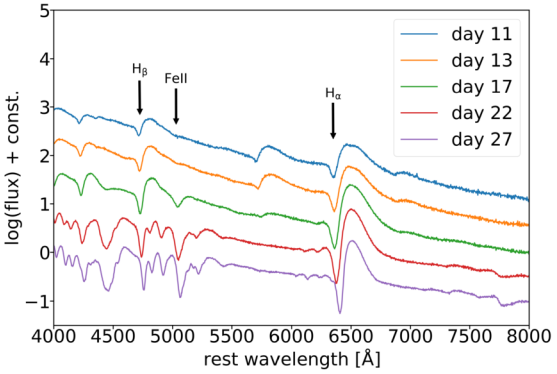


**Fig. 7** Spectral evolution of core-collapse SN1999em based on the TARDIS simulation from Vogl et al. (2019, 2020). Three prominent spectral features, H$\beta$, FeII and H$\alpha$, are labelled. The SN phases are indicated by their rest-frame days after explosion. As the SN phase increases, the spectral features become stronger and the absorption wavelengths increase. Such a sequence of spectra of the first-appearing SN image provides the wavelength-phase relation, and a measurements of the absorption wavelength of a trailing SN image therefore provides information of its SN phase and thus its time delay relative to the first-appearing SN image. With each spectrum of signal-to-noise of 20, Bayer et al. (2021) showed that the time delays can be measured with uncertainties of $\sim 2$ days per spectral feature, even after accounting for the effects of microlensing. Figure taken from Bayer et al. (2021)

plateau phase of this Type IIP SN. The spectra show prominent absorption lines, especially H$\beta$, FeII and H$\alpha$ that are indicated on the figure, and the absorption wavelength increases as a function of time. It is precisely such evolutions in the spectral features that allow us to infer the time delays between two SN images.

In more detail, a sequence of spectra of the first appearing SN image, say SN image A (such as those shown in Fig. 7) yields the absorption wavelength of each spectral feature as a function of the SN phase (days after explosion). When we obtain a single spectrum of a trailing SN image, say SN image B, and measure the absorption wavelength of the same spectral feature, we can determine the phase of SN B by using the relation between the absorption wavelength and phase from SN A. The determined phase of SN B relative to SN A, together with the known observational times of the epochs, then allows us to compute the time delays between SN images A and B. Microlensing of SN introduces scatter in the relation between the absorption wavelength and phase, and this effect can be quantified using microlensing maps such as those from the GERLUMPH software (Vernardos and Fluke 2014; Vernardos et al. 2014, 2015). Accounting for the effect of microlensing that distorts spectra, Bayer et al. (2021) have shown that this technique can yield time delays with uncertainties of $\sim$2 days per spectral feature with signal-to-noise in the spectra of $\sim$20 per wavelength bin of 3Å width. With multiple spectral features and epochs, the inferred time delays from such spectral approach will be even more precise and accurate.

### 2.3 Cosmography with Lensed SNe: Present Cosmological Constraints and Future Forecasts

Of the six known lensed SN systems with spatially resolved SN images, SN Refsdal and SN H0pe with time delays of tens to hundreds of days are suitable in delivering a precise and accurate $H_0$ measurement (with $<10\%$ uncertainty). As mentioned in Sect. 1, the time delay of image SX relative to the first image S1 of SN Refsdal has recently been measured

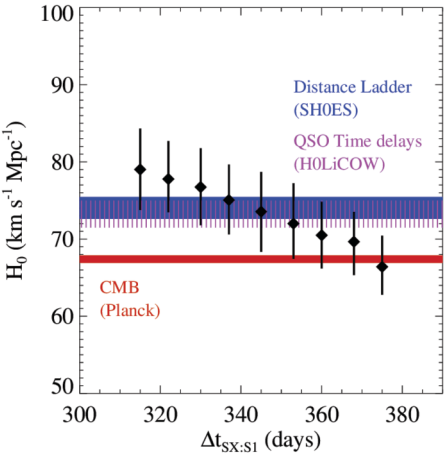


**Fig. 8** Forecast of $H_0$ from SN Refsdal as a function of the time delay between SN images SX and S1, using the reference mass model of Grillo et al. (2020). The median values of $H_0$ (diamonds) with the $1\sigma$ uncertainties in flat $\Lambda$CDM are shown for 9 different hypothetical SX-S1 delays, each with an assumed uncertainty of 10 days. For comparison, the blue, magenta and red bands show, respectively, the $1\sigma$ credible intervals from SH0ES (Riess et al. 2019), H0LiCOW (Wong et al. 2020) and Planck (Planck Collaboration et al. 2020). Figure taken from Grillo et al. (2020)

with 1.5% uncertainty by Kelly et al. (2023b). Combining the time delays with the two best-fitting cluster mass models that are weighted by a selection of observables, Kelly et al. (2023a) obtained $H_0 = 66.6^{+4.1}_{-3.3}\,\mathrm{km\,s^{-1}\,Mpc^{-1}}$. This is in good agreement with the forecast (both in value and uncertainties) shown in Fig. 8 that is taken from Grillo et al. (2020), who predicted the cosmological constraints on $H_0$ for a range of SX time delays before the delay was measured.

Various studies indicate that current and future surveys would discover dozens to hundreds of lensed SNe (Goobar et al. 2002; Oguri and Marshall 2010; Goldstein et al. 2019; Wojtak et al. 2019; Pierel et al. 2021). In particular, Oguri and Marshall (2010) anticipated thousands of lensed quasars and ~100 lensed SNe to be detected in the Rubin Observatory Legacy Survey of Space and Time (LSST; LSST Science Collaboration et al. 2009). Using a mock sample of ~1500 well-observed lenses (consisting of 1476 lensed quasars and 66 lensed SNe) and assuming Planck priors in a flat Universe, Oguri and Marshall (2010) expected the following $1\sigma$ uncertainties on cosmological parameters: $\sigma(w_0) = 0.15$, $\sigma(w_a) = 0.41$ and $\sigma(h) = 0.017$ where $(w_0, w_a)$ are the time-independent and time-dependent components of the dark energy equation-of-state parameter, and $h$ is $H_0$ in units of $100\,\mathrm{km\,s^{-1}\,Mpc^{-1}}$.

Huber et al. (2019) analyzed in detail the number of lensed SNe Ia that could yield time-delay measurements with precisions better than 5% and accuracies better than 1%, with realistic microlensed SN Ia light curves and LSST observing strategies. While LSST is efficient at detecting lensed SNe given its wide survey area and depth, the observing cadence per filter is not rapid enough to map out light curves for precise delay measurements. Follow-up observations at the cadence of at least one epoch every 2 days would drastically increase the number of lensed SNe with "good" time delays (i.e., those delays with uncertainties <5% in terms of precision and <1% in terms of accuracy). Based on the results of Huber et al. (2019), Suyu et al. (2020) simulated a sample of 20 lensed SNe Ia from LSST that are expected to have good time delays. Assuming that these systems would have high-resolution imaging and spatially resolved kinematic measurements to break the mass-sheet degeneracy and yield 6.6% uncertainty on $D_{\Delta t}$ and 5% uncertainty on $D_\mathrm{d}$, this modest sample of 20 lensed SNe Ia could yield constraints on $H_0$ and $\Omega_\mathrm{m}$ of 1.3% and 19%, respectively, in flat $\Lambda$CDM, as illustrated in Fig. 9. In an open $\Lambda$CDM cosmology (i.e., allowing for a spatially curved Universe), a similar constraint on $H_0$ compared to flat $\Lambda$CDM is achievable, while in

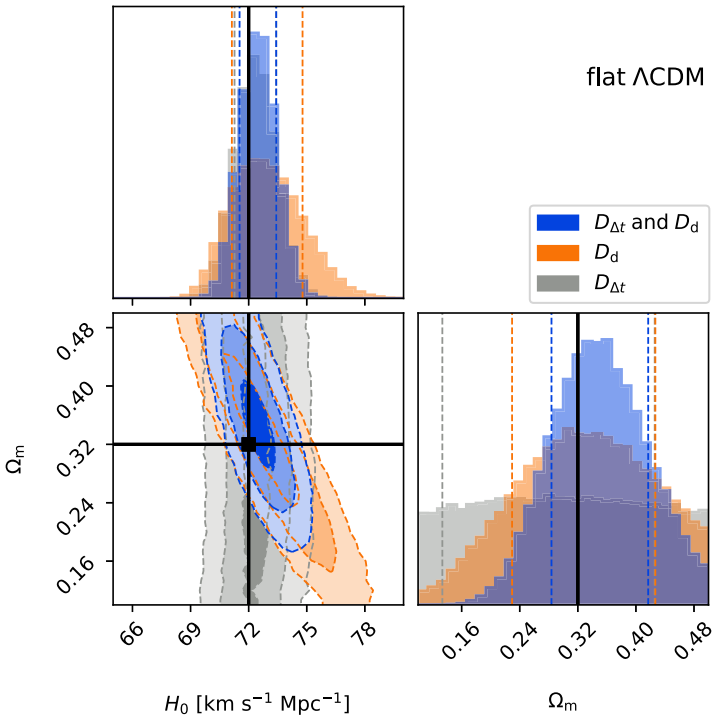


**Fig. 9** Forecast of constraints on $H_0$ and $\Omega_{\rm m}$ in flat ΛCDM from a sample of 20 lensed SNe Ia from LSST with precise and accurate time-delay measurements. Assuming distance measurements of $D_{\Delta t}$ and $D_{\rm d}$ with 6.6% and 5% uncertainties, respectively, for each lensed SN Ia, this modest sample is expected to yield $H_0$ and $\Omega_{\rm m}$ with precisions of 1.3% and 19%, respectively. Figure taken from Suyu et al. (2020)

the flat $w$CDM cosmology (where the dark energy equation-of-state parameter $w$ is allowed to vary), the $H_0$ constraint degrades to 3% (Suyu et al. 2020).

The forecast made by Suyu et al. (2020) did not make use of the standardisable nature of SNe Ia, due to the effects of microlensing and millilensing as mentioned in Sect. 2.1. Nonetheless, Foxley-Marrable et al. (2018) showed that lensed SNe Ia with asymmetric configurations, i.e., with a SN image located far outside the Einstein radius of the foreground lens, have low microlensing scatter of $\lesssim$0.15 mag for the outer SN image, which is comparable to the intrinsic dispersion of a typical SN Ia. These systems are thus standardisable in terms of overcoming microlensing perturbations, and Foxley-Marrable et al. (2018) estimated that about ∼22% of the ∼ 930 LSST systems predicted by Goldstein et al. (2018) would be standardisable. However, Goldstein et al. (2018) estimated that only ∼650 systems would be detected early enough by LSST to deliver reliable time delays. This implies a sample of ∼140 lensed SNe Ia that are standardisable and with potential time-delay measurement.

Following the estimates of Foxley-Marrable et al. (2018) and by making use of 144 standardisable lensed SNe Ia, Birrer et al. (2022) combined non-lensed SNe Ia with lensed SNe Ia via a Bayesian hierarchical framework to infer the constraints on $H_0$. The aim is to use the standardisable nature of SNe Ia to break the mass-sheet degeneracy, without using spatially resolved kinematics of the lens galaxy. Assuming optimistically that the time delays between SN image pairs can be measured with a precision of 2 days for all these systems and

that the typical Einstein radius is $\sim 1''$, Birrer et al. (2022) found that $H_0$ can be measured with an uncertainty of 1.5%.

The various cosmological forecasts depend sensitively on assumptions of follow-up observations in order to classify the SN type, measure the time delays, and acquire high-resolution imaging and spectroscopy. As described in Sect. 2.1, these are necessary for measuring absolute distances to lensed SNe and using them as a cosmological probe. In Sect. 4.4, we discuss in more detail the follow-up requirements for lensed SNe.

## 3 Astrophysical Probe

Lensed SNe are powerful astrophysical tools to study supernovae and galaxies, in addition to probing cosmology through their time delays.

In Sect. 3.1, we explain how lensed SNe provide an excellent opportunity to constrain SN progenitors. In Sect. 3.2, we describe how lensing magnifications enable the acquisition of high-redshift SN spectra that are crucial for SN cosmology. In Sect. 3.3, we outline the use of microlensing to probe SN structure. In Sect. 3.4, we show lensed SNe as a probe of dust in the foreground lens galaxy.

### 3.1 SN Physics and Progenitors

Whilst it is accepted that a Type Ia SN is a thermonuclear detonation of a white dwarf (WD), the cause of the detonations remains uncertain even after decades of study (Maoz et al. 2014; Livio and Mazzali 2018).

The classic progenitor model (often referred to as the single degenerate channel) for a Type Ia SN is a close binary of a white dwarf and a post main sequence star (Whelan and Iben 1973). As the star expands, it overflows its Roche lobe and its outer layers are accreted onto the WD until the WD reaches the Chandrasekhar mass. At this point, electron degeneracy pressure can no longer support the WD, and gravitational collapse causes thermonuclear detonation of the WD. This model is attractive, since it naturally explains the standardisability of SNe Ia, with the progenitor always having the same mass and near identical composition. However the lack of evidence for surviving companions suggest that this channel cannot account for all SNe Ia (González Hernández et al. 2012; Lundqvist et al. 2015).

An alternative progenitor model is the double degenerate channel. Here two white dwarfs merge, exceeding the Chandrasekhar mass (Iben and Tutukov 1984; Webbink 1984). This mechanism leaves behind no companion star, but since each pair of white dwarfs will sum to a different mass, there is no obvious reason why this channel would produce a good standard candle. In addition to these two classic channels of single- and double-degenerate systems, there are other explosion mechanisms that have been explored, including sub-Chandrasekhar explosions (e.g., Sim et al. 2010), delayed detonations (e.g., Röpke et al. 2012), and double detonations of sub-Chandrasekhar WDs (e.g., Fink et al. 2007).

Early observations of SN light curves are critical in constraining the properties of SN progenitor systems (e.g. Kasen 2010, Piro et al. 2010, Rabinak and Waxman 2011, Nugent et al. 2011, Bloom et al. 2012, Goobar et al. 2015, Piro and Morozova 2016, Noebauer et al. 2017, Kochanek 2019, Fausnaugh et al. 2021, Yao et al. 2019, Miller et al. 2020, Bulla et al. 2020). If non-degenerate matter is close to the WD, then it should be shock heated by the explosion, producing excess high energy flux in the first few hours to days of the light curve. In addition to SNe Ia, early observations of core-collapse SNe are also helpful in

constraining the properties, such as the sizes, of the progenitor stars (e.g., González-Gaitán et al. 2015; Chen et al. 2022). Even with the development of wide-field optical surveys, observing these earliest moments of SNe is heavily reliant on chance. Strong lensing gives us the opportunity to predict the precise reappearance time of a SN, such that very early data can be gathered (Suwa 2018; Suyu et al. 2020).

There are multiple challenges to this approach: early detection of the first SN image, possible image demagnification, distortions of SN light curves and spectra by microlensing, and time delay predictions of insufficient precision. We discuss each of these in turn.

Detection of a lensed SN based on only the appearance of the first image is more difficult, due to possible confusions between a lensed and an unlensed SN without the multiple SN images present. This confusion can be overcome when the lensed SN host galaxy is visible as lensed arc features in addition to the foreground lens galaxy.

Whilst lensed SNe will be discovered from highly magnified images, images occurring with significant time delay after the bright "discovery image" are typically demagnified in the case of two-image systems (Foxley-Marrable et al. 2020). The situation is better for four-image systems where some of the trailing SN images can be brighter than the discovery SN image. We expect $\sim 2/3$ of the lensed SNe to be two-image systems, and $\sim 1/3$ to be four-image systems (Oguri and Marshall 2010).

As seen in Fig. 4 and shown in Huber et al. (2019), microlensing distorts the SN light curves and spectra, potentially garbling the information on progenitors. Encouragingly, Suyu et al. (2020) have investigated the microlensing effects on four different explosion models of SNe Ia and demonstrated that spectral distortions due to microlensing are $\lesssim 1\%$ at the $1\sigma$ level within 10 rest-frame days after explosions. Therefore, microlensing is expected to have negligible impact on early-phase spectra (within $\sim$10 rest-frame days) for deciphering SN progenitors.

Finally, time delays cannot be precisely estimated from lens modelling alone. A 5-10 percent precision is typical from the best lens models (e.g., Shajib et al. 2019), and the uncertain value of the Hubble constant given the discrepant $H_0$ measurements (e.g., Verde et al. 2019; Di Valentino et al. 2021) adds several more percent of uncertainty in the predicted time delays. For systems with delays $\gtrsim 20$ days that are sufficiently long to catch the trailing SN images from their beginnings (given the time it takes to detect the first SN image and to arrange follow-up observations), a 10% uncertainty would translate to $\gtrsim 2$ days. Given this uncertainty, the predicted delay can easily miss the observations within $\sim 2$ days after explosion, the crucially early moments for constraining SN progenitors.

To overcome these challenges, deep and high-cadence (ideally daily) monitorings with imagers after the detection of the first appearing SN image would greatly help. Such a monitoring would acquire the early-phase light curves of trailing SN images, and spectroscopic observations of the early phases can be triggered as soon as a trailing SN image appears in the monitoring. Early-phase spectroscopic observations especially in the rest-frame UV are unprecedented and important for constraining SN progenitors (Suyu et al. 2020). The time delays of lensed SNe provide a unique and exciting avenue to acquire such spectroscopic observations for studying SN progenitors.

### 3.2 High-Z SN Spectra Through Gravitational Telescopes

The precision of SNe Ia as distance indicators, and thus their use to accurately constrain the nature of dark energy, is ultimately limited by our understanding of progenitor systems, e.g., the potential evolution of the SN properties, especially their absolute magnitude, over cosmic time. Thus, confirming the standard-candle nature through spectroscopic comparisons

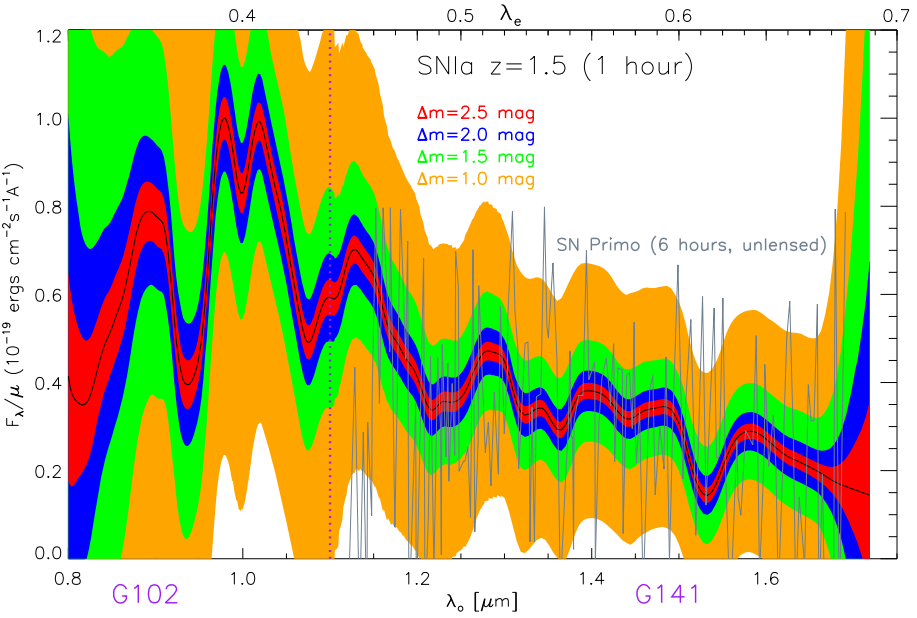


**Fig. 10** Expected signal for HST observations through grisms G102 and G141 of a SN Ia at $z = 1.5$ for different magnifications provided by lensing. The shaded regions in [orange, green, blue, red] indicate the $1\sigma$ uncertainty per pixel in one-hour-long exposures for $\Delta m = [1, 1.5, 2.0, 2.5]$ mag of magnification, respectively. The observed spectrum of "SN Primo" (Rodney et al. 2012, six hours exposure time) is also shown for comparison

between SNe near and far is essential. With current instruments, detailed comparisons beyond $z > 1$ are not possible, due to the low SNR. This will remain challenging in the JWST era. However, multiple spectra of SNe at high redshift are required to check if the progenitor population evolves with redshift. Hence, the magnification of the signal from gravitational lensing could become essential to constrain one of the biggest systematic uncertainties in SN Ia cosmology (Petrushevska et al. 2017; Johansson et al. 2021). Figure 10 shows the noisy HST spectrum, based on six hours of observations of SN "Primo" at $z = 1.55$ observed by Rodney et al. (2012) compared with the expected signal if observed for shorter time through gravitational telescopes of different strengths, $\Delta$m = 1, 1.5, 2.0 and 2.5 mag, where $\Delta$m is the difference in magnitude coming from lensing magnification. These magnifications are expected to be typical for lensed SNe (Goldstein et al. 2019).

### 3.3 SN Structure with Microlensing

When a background source crosses a caustic network produced by microlenses, this allows one to estimate the physical dimensions of the light emitting surface, most robustly its half-light radius (Mortonson et al. 2005; Vernardos and Tsagkatakis 2019). For the case of SNe, their expanding ejecta lead to an increasing size that is directly linked to the expansion velocity. Because the (unobservable) distance from a caustic/high magnification region on the source plane is inversely proportional to changes in brightness due to microlensing, deformed SN light curves, like the ones shown in Fig. 4, can be used to constrain the size evolution, and subsequently the expansion velocity. In combination with the measurements

of the photospheric velocity of the SN ejecta from spectroscopic observations, the SN size evolution can provide information on SN explosion models. Furthermore, microlensing is a potential way to probe asymmetries in the SN photosphere, since each of the multiple SN images will have different parts of its photosphere being microlensed.

We illustrate the size measurement via microlensing by the following toy model. Let us assume that the brightness of a lensed SN image at any given time $t$ and wavelength $\lambda$ (ignoring time delays and macromagnification for simplicity) is:

$$I(t,\lambda) = \int \mathrm{d}x \int \mathrm{d}y\, S(x,y;t,\lambda)\, \mu(x,y), \tag{6}$$

where $S$ is the two dimensional intrinsic SN brightness profile, $\mu$ is the microlensing magnification on the source plane, and the integrals are performed over the extent of the source brightness profile. Assuming, for illustrative purposes, that the intrinsic surface brightness profile ($S$) is a circle of radius $R(t)$ with a known, constant surface brightness $i(t,\lambda)$, we get:

$$I(t,\lambda) = i(t,\lambda) \int_0^{2\pi} \int_0^{R} \mu(r,\theta)\, r\, \mathrm{d}r\, \mathrm{d}\theta = i(t,\lambda) F(R) \tag{7}$$

in polar coordinates $(r,\theta)$, where the value of the integral can be written as a radius and time-dependent factor, $F(R)$, and whose probability distribution can be calculated numerically from magnification maps. In fact, we can drop the assumption on a uniform profile and perform the convolution in Eq. (6) for different profile shapes. Therefore, if we know $S(x,y;t,\lambda)$ from a standardised SN type and calculate $F$, then we can measure $R(t)$. If the SN brightness profile shape varies over time, ratios of $I(t,\lambda)$ can be considered for separations in time $\Delta t$ small enough so that the profile does not change by much. Finally, we note that Dobler and Keeton (2006) have used a similar approach, the time-weighted light curve derivative, albeit to measure the stellar mass fraction of the lensing galaxy.

In an analogous way, the relative size, or more specifically the half-light radius, of the SN ejecta at different wavelengths can be estimated from Eq. (6). Actually, the shape of the SN profile and/or the expansion velocity may vary in different wavelengths (see Figs. 11 and 12; Huber et al. 2019; Bayer et al. 2021), leading to different half-light radii (i.e., $R = R(t,\lambda)$ instead of $R(t)$). In the context of our toy model, the brightness ratio between two wavelengths at a given time $t$ can be used to constrain the relative half-light radii:

$$\frac{I(t,\lambda_1)}{I(t,\lambda_2)} = \frac{i(t,\lambda_1)}{i(t,\lambda_2)} \frac{F(R_1)}{F(R_2)}. \tag{8}$$

Such measurements of radii across wavelengths and time not only provide a check on whether the expansion is homologous (when comparing the radii to the measured velocities from spectra), but also information on the explosion models that alter the dependence of radius on wavelength. It remains to be seen whether microlensing constraints on explosion models are competitive to the existing constraints based on SN spectral evolution modelling and analysis.

### 3.4 Dust Properties in Distant Galaxies

The different sightlines of multipe images offer unique opportunities to explore the properties of the interstellar medium of the deflecting galaxy, as was first shown for strongly

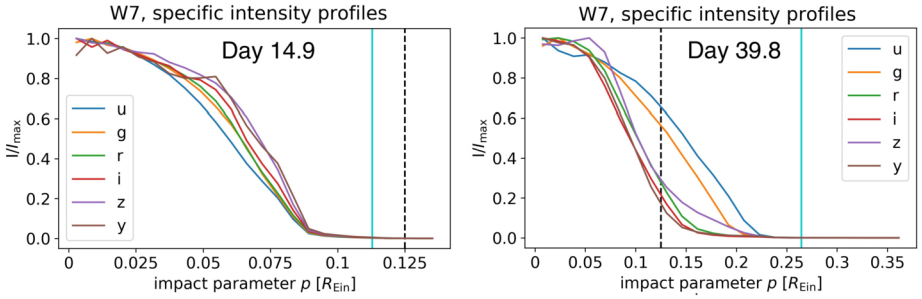


**Fig. 11** Specific intensity profile of the W7 explosion model of SNe Ia. Left: radial intensity profiles in different filters 14.9 rest-frame days after explosion, in units of the Einstein radius of the microlenses ($R_{\rm Ein} = 2.2 \times 10^{16}$ cm for this specific case). The vertical solid cyan lines indicate the radius that encloses 99.9% of the total projected specific intensity. The vertical black dashed lines are random locations of caustics – effects of microlensing are strong when the specific intensity of the SN crosses a caustic. Right panel: same as the left panel but for a SN Ia 39.8 rest-frame days after explosion. Figure extracted and modified from Huber et al. (2019)

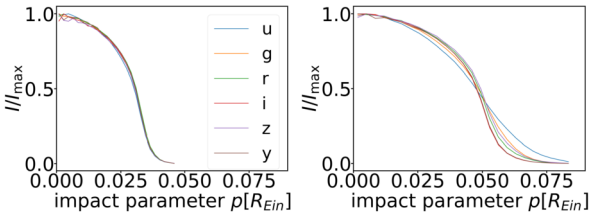


**Fig. 12** Specific intensity profiles from TARDIS (Kerzendorf and Sim 2014; Vogl et al. 2019) modelling of SN 1999em, a Type IIP SN (Vogl et al. 2020) projected on the plane of the sky (Bayer et al. 2021). Left: radial intensity profiles in different filters 11 rest-frame days after explosion, in units of the Einstein radius of the microlenses ($R_{\rm Ein} = 2.9 \times 10^{16}$ cm for this specific case). Right panel: same as the left panel but for 27 rest-frame days after explosion. Figure taken from Bayer et al. (2021)

lensed QSOs by Falco et al. (1999) and in subsequent studies (e.g., Elíasdóttir et al. 2006; Østman et al. 2008; Hjorth et al. 2013). This is important as accurate measurements of e.g., the total-to-selective extinction parameter $R_V \equiv A_{\rm V}/E(B-V)$, a key number for many areas of astronomy, are very hard to establish outside the Milky Way and the Magellanic Clouds. The *extinction* in the V-band, $A_{\rm V}$, is defined as

$$A_{\rm V} := m_{\rm V} - m_{\rm V,0}, \tag{9}$$

where $m_{\rm V}$ is the apparent magnitude with dust extinction and $m_{\rm V,0}$ is the intrinsic magnitude without dust extinction. The extinction for any other wavelength band is defined in a similar way. The *color excess* (or reddening) between the B and V band is

$$E(B-V) := A_{\rm B} - A_{\rm V} \tag{10}$$

$$= (m_{\rm B} - m_{\rm V}) - (m_{\rm B,0} - m_{\rm V,0}). \tag{11}$$

In the case of no dust extinction, then $A_{\rm V} = 0$, $A_{\rm B} = 0$ and $E(B-V) = 0$. For a fixed $R_{\rm V}$ value, higher $A_{\rm V}$ values (or higher $E(B-V)$ values) correspond to more dust along the sightline. The observed colors in multiple bands of the images are used to infer the

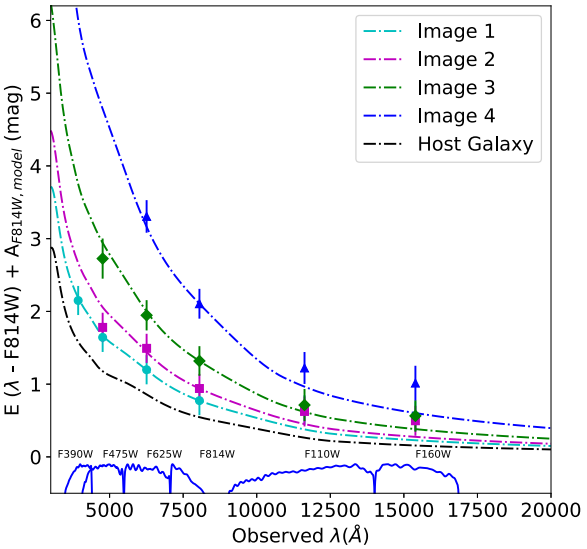


**Fig. 13** The observed color excess for the resolved images from HST of iPTF16geu as a function of wavelength. The absorption from the host galaxy dust grains is plotted in black. For Image 1 we can see that the host galaxy is the dominant source of extinction, and for images 2, 3, 4 there is a progressively larger contribution from the dust in the lens galaxy, with correspondingly higher values of the color excess. Figure taken from Dhawan et al. (2020)

differential reddening as the various images travel through different regions of the lensing galaxy (i.e., infer the differences in $A_V$ between the multiple SN images). Multi-wavelength observations of the lens system will also allow one to probe variations in $R_V$ for different sightlines traversed by the multiple SN images (our own Milky Way shows variations in $R_V$; Fitzpatrick and Massa 2007; Schlafly et al. 2016). Corrections for differential extinctions in systems of strongly lensed SNe Ia is crucial to also make use of their standard candle nature to infer the lensing magnification.

Exploiting the well-known color evolution of SNe Ia, Dhawan et al. (2020) were able to infer both the extinction in the lensing galaxy for iPTF16geu, along with the common color excess from attenuation in the host galaxy using multi-band images from HST, as shown in Fig. 13. For iPTF16geu, with an impact parameter of about 1 kpc, two of the images (3 and 4) suffered significant extinction and the total magnification inferred from spatially unresolved images was significantly underestimated. Intriguingly, the best fit values of $R_V$ for the lensing galaxy at $z = 0.216$ were much lower than what is observed for studies of stars in the Milky-Way (Schlafly et al. 2017), but similar to what is found in studies of well-measured, highly-reddened SNe Ia (Amanullah et al. 2015).

## 4 Searches and Rates

### 4.1 Methods

There are multiple ways to find lensed supernovae by making use of their image morphology, magnification, image multiplicity and/or time evolution. We briefly describe several approaches in this subsection.

#### 4.1.1 Search Through Known Lensed Galaxies

A straightforward approach to find lensed SNe is to monitor known lensed galaxies and wait for a SN to explode in one of the lensed galaxies (Shu et al. 2018a). Using the sample of 128

galaxy-scale strong-lens systems from the Sloan Lens ACS Survey (SLACS; Bolton et al. 2006, 2008), the SLACS for the Masses Survey (S4TM; Shu et al. 2017), and the Baryon Oscillation Spectroscopic Survey Emission-Line Lens Survey (BELLS; Brownstein et al. 2012; Bolton et al. 2012), Shu et al. (2021, 2018a) estimated that the rates of strongly lensed SNe Ia and core-collapse SNe are $0.34 \pm 0.03$ and $2.8 \pm 0.2$ events per year, respectively.

One can either monitor known lens systems (especially ones with the highest star-formation and SN rates) through dedicated observing programs (Craig et al. 2021), or through wide-field imaging surveys such as the ongoing ZTF (Bellm et al. 2019). In the latter case, lens systems and lens candidates can be cross matched to transient alerts from ZTF through various brokers such as AMPEL (Nordin et al. 2019), ANTARES (Saha et al. 2014; Narayan et al. 2018; Lee et al. 2020; Matheson et al. 2021) and Lasair (Smith et al. 2019). Multi-epoch images of lens candidates can also be used to find lensed SNe based on temporal and spatial information of transients occurring near the lens candidates (Sheu et al. 2023). There are now thousands of confirmed and candidate lens systems from a wide range of lens searches, notably through machine learning approaches in recent years (e.g., Bolton et al. 2006; Limousin et al. 2009; Gavazzi et al. 2012; Brownstein et al. 2012; Vieira et al. 2013; Cañameras et al. 2015; Jacobs et al. 2017, 2019; Marshall et al. 2016; More et al. 2016; Sonnenfeld et al. 2018, 2020; Petrillo et al. 2019; Cañameras et al. 2020, 2021; Huang et al. 2020, 2021; Savary et al. 2022; Rojas et al. 2022; Shu et al. 2022; Tran et al. 2022). However, given the relatively shallow limiting depth of $r = 20.6$ mag ($5\sigma$) of the ZTF survey (Bellm et al. 2019), individual lensed SN images associated with the lensed galaxies are likely below the detection threshold (Oguri and Marshall 2010; Wojtak et al. 2019). Nonetheless, the combination of the flux from all lensed SN images can be above the detection threshold, which motivates the next search approach through magnifications.

#### 4.1.2 Search Through Lensing Magnification

While targeted searches for lensed SNe in known strongly lensed systems is straightforward, it is also constraining given the limited number of such systems. Since supernovae, especially SNe Ia, have a known narrow range of intrinsic brightness, it is feasible to identify particularly bright SNe as potential lensing candidates.

Quimby et al. (2014) proposed a technique to find unresolved lensed images of SNe Ia based on their high magnification and colors. Lensed SNe are expected to come from high redshifts where they will be in larger numbers owing to a larger volume and the lensing probability being higher for distant sources. The lensing magnification will make them appear brighter but their colors will largely be unaffected. Hence, in a color-magnitude diagram, the lensed SNe Ia will appear redder, at given magnitude, since they will be originating from higher redshifts compared to the unlensed population (see the blue circles above the black solid line in Fig. 14). Subluminous SNe, such as SN 1991bg, tend to be red as well (e.g., Miller et al. 2017) and would contaminate lensed SN candidates selected via this color-magnitude approach.

Another technique is based on having some knowledge of the redshifts of the galaxies involved, and it is interesting since it does not require multiple images to be spatially resolved. Thus it can in principle be used to detected arbitrarily compact systems, complementing other techniques, and allowing to probe the entire angular separation distribution of strongly lensed systems.

Figure 15 from Goobar et al. (2017) shows a practical realisation of detecting unresolved strongly lensed supernova: iPTF16geu was found to be a $30\sigma$ outlier when compared with other SNe Ia at the same redshift. Thus, even with the very modest $\sim 2''$ spatial resolution

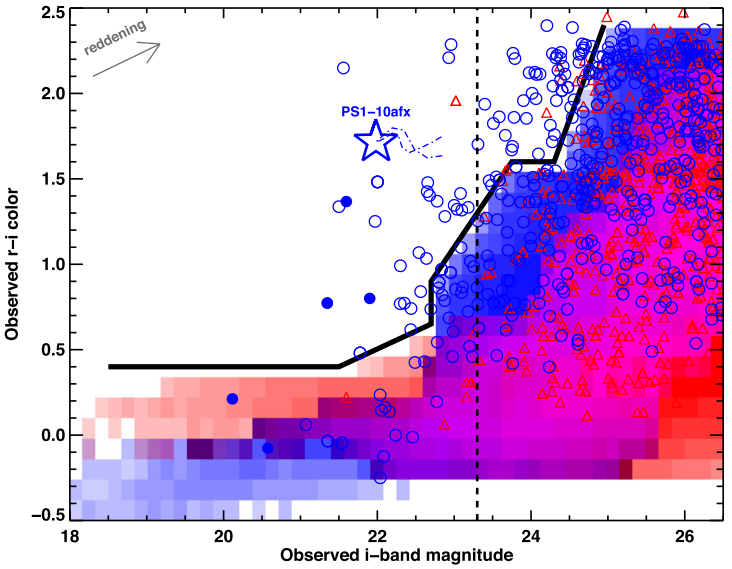


**Fig. 14** The expected distribution of unlensed SNe population (SNe Ia in blue shaded, and core-collapse SNe in red shaded) is enclosed by thick black line showing the red limit. The lensed population predicted by Monte Carlo simulations is shown for SNe Ia (blue circles) and core-collapse SNe (red triangles). Vertical line marks the single epoch limit for LSST. Figure taken from Quimby et al. (2014)

at the 48-inch telescope at the Palomar Observatory, a strongly lensed system with $\theta_E = 0.3''$ could be identified. The difficulty with this approach is that spectroscopic observations are needed for classification of the transients, along with obtaining reliable redshifts of the galaxies, potentially a daunting task for large surveys with tens or even hundreds of new astrophysical transients found every night.

Goldstein and Nugent (2017) proposed a methodology to lower the rate of false positives: only considering transients spatially associated with elliptical galaxies, which make up about $\sim 80\%$ of the galaxy lenses and typically only host SNe Ia, including the sub-luminous ones. Furthermore, thanks to prominent 4000Å breaks, robust photometric redshifts can be computed for elliptical galaxies. Hence, if the transient appears to be too bright for being a SN Ia at the (photometric) redshift of the nearest galaxy, there is a good chance that it is a deflecting galaxy, as opposed to the host. Upon a secure identification, targeted high spatial-resolution imaging can be used to try to resolve the system.

### 4.1.3 Search Through Multiplicity of Images

For imaging surveys with faint limiting depth and good angular resolution such as the upcoming LSST, the multiple SN images of a lensed SN can be resolved and detected individually. Oguri and Marshall (2010) and Wojtak et al. (2019) investigated the number of lensed SNe detectable from such an approach. Specifically, Wojtak et al. (2019) imposed the following conditions for detecting a lensed SN via its image multiplicity: (1) the maximum image separation between the multiple SN images is between $0.5''$ and $4''$, where the lower limit is set by the expected seeing of LSST and the upper limit puts focus on galaxy-scale lens systems, (2) the flux ratio between the two images of a two-image (double) system is larger than 0.1, in order to have good contrast and clear identification of the images, and (3)

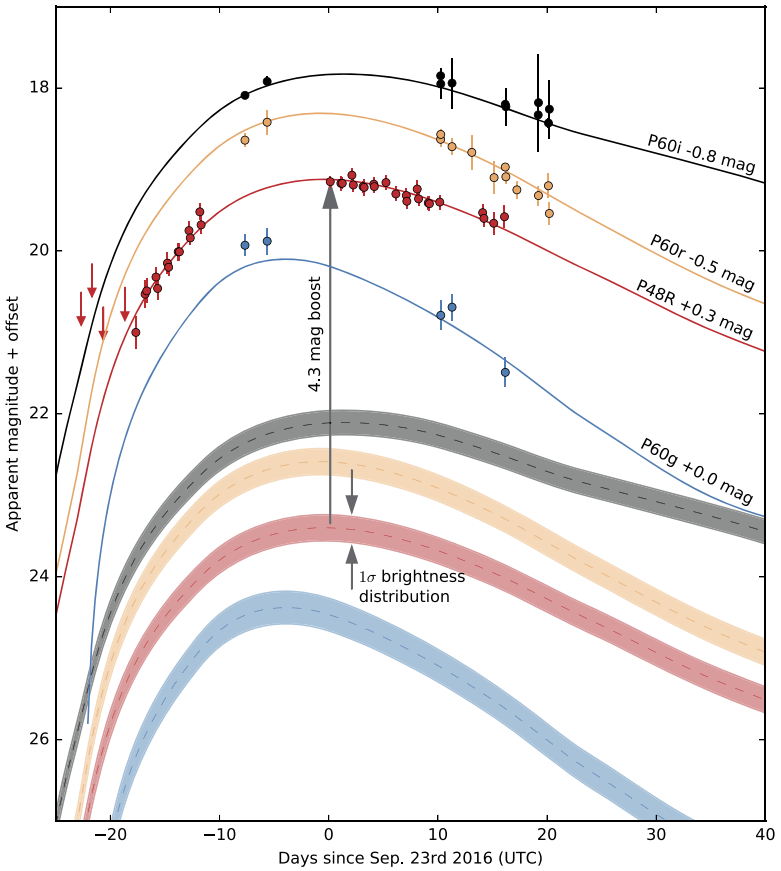


**Fig. 15** Multicolor light curve of iPTF16geu showing that the unresolved supernova was 4.3 magnitudes (30 standard deviations) brighter than expected for its redshift. The magnitudes are measured with respect to time of maximum light in the R-band at P48 and in the g-, r-, and i-bands with the P60 telescope. The solid lines show the best-fitted SN Ia model to the data, while the dashed lines indicate the expected light curves at $z = 0.409$ (without lensing). The bands represent the standard deviation of the brightness distribution for SNe Ia. To fit the observed light curves, a brightness boost from gravitational lensing of 4.3 magnitudes is required. Figure from Goobar et al. (2017)

at least three of the four images in a quad system are detected, and both images of a double system are detected.

For surveys with limiting magnitude that are fainter than ∼23 mag in g, r or i-band, the detection via image multiplicity is expected to detect more lensed SN systems than the magnification approach. We illustrate this in Fig. 16 for lensed SNe Ia, and refer to Wojtak et al. (2019) for other types of lensed SNe that show similar trends. A combination of the two complementary approaches (magnification and multiplicity), as labelled by "hybrid" in Fig. 16, delivers more lens systems than the individual approaches on their own. In terms of cosmological applications, the multiplicity approach tends to detect lensed SN systems with longer time delays and larger image separations, which are more suitable for time-delay cosmography.

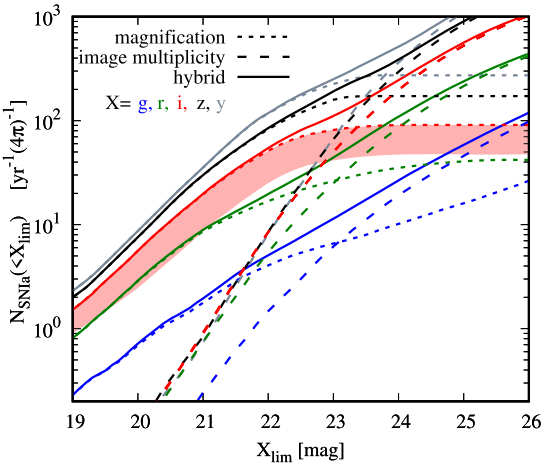


**Fig. 16** The number of lensed SNe Ia expected per year over the whole sky as a function of the imaging survey limiting magnitude depth. The different colors correspond to detection in different filters (g, r, i, z or y). The dotted (dashed) lines show the expected number of lensed SNe Ia detected through the magnification (image multiplicity) approach. The hybrid approach, a combination of magnification and image multiplicity, is indicated by the solid curve. For shallow image surveys with limiting depth brighter than ∼22 such as the ZTF survey, the magnification approach dominates in providing most of the expected lensed SNe. For deep image surveys with limiting depth fainter than ∼23 such as the LSST survey, the image multiplicity approach start to dominate. Figure taken from Wojtak et al. (2019)

### 4.1.4 Search Through Spatio-Temporal Images

Most of the lensed SN searches in ZTF are based on the approaches of cross matches to lens systems/candidates (Sect. 4.1.1) or magnification (Sect. 4.1.2) since the angular resolution of ZTF (with 1″ pixel sizes) does not resolve the multiple SN images of typical lens systems. However, in the advent of LSST, there will be high angular-resolution and deep images with at least hundreds of epochs per filter at each sky location. Building upon the image multiplicity method described in Sect. 4.1.3, Kodi Ramanah et al. (2022) proposed a machine-learning approach to classify an object based on images from cadenced surveys like the Young Supernova Experiment (YSE; Jones et al. 2021) and LSST. Machine learning techniques such as convolutional neural networks (CNN) perform well and are efficient at processing large amounts of imaging data for finding gravitational lenses (e.g., Jacobs et al. 2017, 2019; Lanusse et al. 2018; Metcalf et al. 2019; Petrillo et al. 2019; Cañameras et al. 2020, 2021). The spatio-temporal method of Kodi Ramanah et al. (2022) builds upon the success of the CNN and incorporate also time-domain information.

Rather than providing a neural network with the multi-band stacked (static) images of objects for classification, Kodi Ramanah et al. (2022) developed a network to take in a temporal series of images. The network architecture is a CNN that encodes long short-term memory (LSTM, a type of recurrent network; Sherstinsky 2020). The concept is that the temporal series of images will show the multiple SN images appearing at different epochs. Even if the multiple SN images are not well resolved, the centroids of the distribution of light would change as the multiple SN images brighten and dim at different times. Such change in the features of the object helps the neural network to distinguish lensed SN (with multiple SN images) from non-lensed SN (with single SN image). Using simulated images of YSE, Kodi Ramanah et al. (2022) demonstrated that the spatio-temporal network improves the

classification accuracy by ∼20% compared to networks that use static (e.g., single-epoch) images. The new development spatio-temporal network is very promising for application to the LSST.

#### 4.1.5 Search Through Light Curves of Unresolved Multiple Images

For lens systems with small image separations between the multiple SN images or poor seeing conditions, the multiple images of the SN will be blended together. The light curve from such an "unresolved" lensed SN system will, therefore, be a superposition of the light curves of the individual SN images.

Bag et al. (2021) developed a new method that uses an orthogonal basis expansion around a trial light curve to fit an observed light curve in order to 1) determine whether the light curve is stemming from a lensed SN, and if so, 2) measure the time delays from the blended light curve. Therefore, the method is independent of any SN model assumptions. When tested on unresolved lensed SN Ia systems with two images, the method could accurately classify and measure the time delays from the blended light curves that have a time delay greater than 10 days. For systems with shorter delays, the method was unable to discern or infer the time delays robustly.

Denissenya and Linder (2022) have further expanded on this approach. They use a CNN (convolutional neural network), instead of the forward modeling approach, to determine the number of multiple (delayed) light curves that constitute a given observed light curve. A resulting value of one means that the light curve is not from a lensed SN, whereas a value of two or more indicates that the light curve stems from a lensed SN with two or more blended images. Using the CNN, Denissenya and Linder (2022) can accurately classify blended light curves coming from lensed SN Ia systems with time delays systematically longer than ∼6 days and measure their delays with an uncertainty of ∼1 day.

Both the studies of Bag et al. (2021) and Denissenya and Linder (2022) have not included microlensing effects, which are deferred to future work. Nonetheless, these first studies based on light curves show promise in finding lensed SNe with blended SN images.

### 4.2 Expected Number of Lensed SN Events

Strongly lensed transients are very rare. Hence, deep, wide-field time-domain optical and Near-IR surveys have the best chances to find samples of lensed SNe. Among these, the (optical) LSST survey at the Vera C. Rubin Observatory to see first light in ∼2025, and the (NIR) Roman satellite, planned for launch some years later offer the best opportunities. In both cases, between several tens to hundreds of strongly lensed supernovae may be expected throughout the multi-year surveys (Goobar et al. 2002; Oguri and Marshall 2010; Quimby et al. 2014; Goldstein et al. 2019; Wojtak et al. 2019; Pierel et al. 2021). The cumulative number of SNe, Type Ia and core-collapse, expected to be found every year by LSST as a function of the detection threshold is shown in Fig. 17. A potential concern is the low cadence of the observations, which may require follow-up observations to measure time delays accurately (Huber et al. 2019).

### 4.3 Expected Lens Properties

Figure 18 shows simulations by Goldstein et al. (2019) of the distribution of system properties for strongly lensed SNe Ia in the LSST survey. The typical source redshift is $z_s \sim 0.9$ with time delays between 2 and 3 weeks. With a median image separation close to $1''$ and the expected good seeing conditions at the Rubin Observatory coupled with the plate-scale of the camera, most events would be spatially resolved.

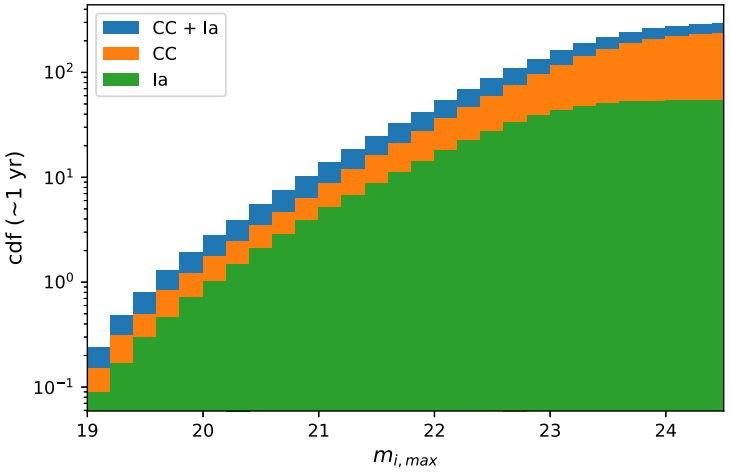


**Fig. 17** Cumulative number of lensed Type Ia and core-collapse supernovae detections by the LSST survey per year as a function of their peak $i$-band magnitude, as computed in Goldstein et al. (2019). Figure credit: Ana Sagués Carracedo

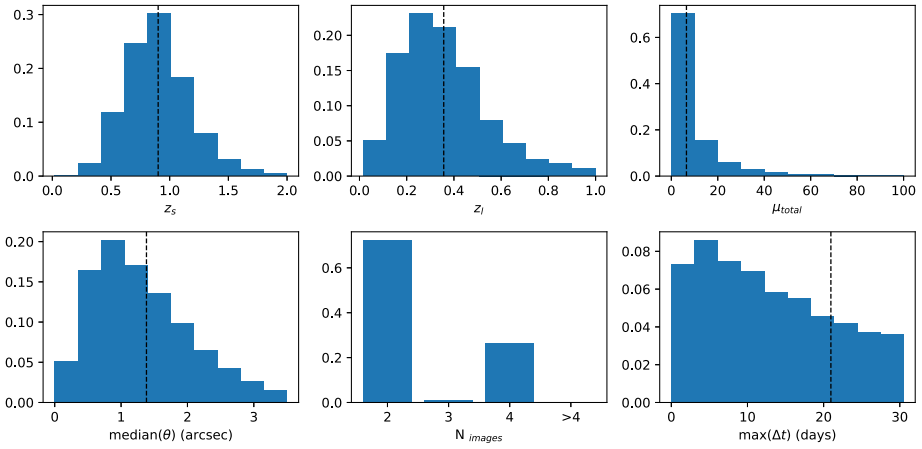


**Fig. 18** Predicted system configurations for strongly lensed Type Ia supernovae in LSST as computed in Goldstein et al. (2019). Figure credit: Ana Sagués Carracedo

### 4.4 Requirements on Follow-up Observations

Full scientific exploitation of strongly lensed SNe depends on 1) early transient detection, ideally well before light curve peak; 2) rapid spectroscopic classification of the transient; 3) well-sampled, spatially resolved light curves; and 4) good wavelength coverage, necessary for accurate extinction corrections. From Fig. 17 one can see that the vast majority of the lensed SNe in forthcoming surveys will have (summed) peak magnitudes fainter than 21 mag. Hence, spectroscopic classification requires 8-m class telescopes, in most cases, potentially a major challenge. As argued in Sect. 3.4, an accurate measurement of the image magnifications requires a wide lever arm in wavelength coverage of the spatially resolved

images, for at least a handful of epochs along the light curve. The new space telescope, JWST, would be ideally suited for follow-up. Its Near-IR sensitivity is an excellent match to the source redshifts shown in Fig. 18.

## 5 Summary

The first discoveries of strongly lensed SNe in recent years are opening a new window of exploration for cosmological and astrophysical studies. In this review, we have provided an overview of the analysis and results from these first lensed SN systems, and the future prospects for this exciting new field. The main takeaway points are as follows.

- There are currently six published strongly lensed SN systems with spatially resolved SN images. Four systems are lensed by galaxy clusters and two lensed by individual galaxies.
- Time delays between the multiple SN images of a lensed SN allow direct measurements of (1) the time-delay distance, (2) the angular-diameter distance to the lens in the case where stellar kinematic measurements of the lens galaxy are available, and (3) the luminosity distance in the case of a Type Ia SN that is a standardisable candle, as long as the SN magnifications due to microlensing and millilensing can be accurately accounted for. These distance measurements provide competitive constraints on cosmological parameters, particularly $H_0$.
- Several new methods to infer the time delays of lensed SNe have been developed in recent years, employing different kinds of data such as light curves, color curves or spectral evolution of SNe. Time-delay measurements with uncertainties of $\sim$1 day are achievable with real and mock data. The fractional uncertainty in the delays contribute directly to the fractional uncertainty on the time-delay distance and the lens angular-diameter distance.
- SNe Refsdal and H0pe are promising for delivering competitive $H_0$ measurements, and the first measurement from SN Refsdal with $\sim$6% uncertainty has been obtained. We expect that a modest sample of 20 lensed SNe Ia from the upcoming LSST to yield $H_0$ with nearly 1% precision in flat $\Lambda$CDM cosmology.
- The time delays of lensed SNe provide a unique opportunity to acquire very early-phase observations of SNe, especially in the rest-frame UV, and probe SN progenitors.
- Lensing magnifications allow the acquisition of spectra of SN above $z > 1$, that are crucial to reduce systematic uncertainties in SN Ia cosmology.
- Microlensing of SNe provides an avenue to constrain the sizes of the SN at different wavelengths.
- The dust properties in the (foreground lens) galaxies can be measured through the multiple SN sight lines in lensed SN systems.
- Various methods have been developed to search for lensed SNe, through e.g., the monitoring of known lens systems, magnification, image multiplicity, spatio-temporal evolution in the imaging, and light curves of unresolved SN images. Depending on the selection criteria, we expect at least dozens of lensed SNe to explode in the upcoming LSST, with their properties summarized in Sect. 4.3.

We are entering a new era of lensed SNe with the upcoming wide-field cadenced imaging surveys. Rapid follow-up observations including spectroscopic typing and light curve monitoring, will be crucial and necessary to make the best use of such events for cosmological and astrophysical studies.

**Acknowledgements** We thank Luke Weisenbach for producing Fig. 5, and Satadru Bag, Raoul Cañameras and Paul Schechter for discussions and feedback on the manuscript. We also thank the two anonymous reviewers for their constructive comments that improved our article. We are grateful to the International Space Science Institute (ISSI) in Bern for the hospitality and the stimulating workshop on "Strong Gravitational Lensing". SHS thanks the Max Planck Society for support through the Max Planck Research Group and the Max Planck Fellowship.

**Funding** Open Access funding enabled and organized by Projekt DEAL. This project has received funding from the European Research Council (ERC) under the European Union's Horizon 2020 research and innovation programme (LENSNOVA: grant agreement No 771776). This research is supported in part by the Excellence Cluster ORIGINS which is funded by the Deutsche Forschungsgemeinschaft (DFG, German Research Foundation) under Germany's Excellence Strategy – EXC-2094 – 390783311. AG acknowledges support from the Swedish National Space Board and *Vetenskapsrådet*, the Swedish Research Council. TEC is funded by a Royal Society University Research Fellowship. GV has received funding from the European Union's Horizon 2020 research and innovation programme under the Marie Sklodovska-Curie grant agreement No 897124. GV's research was made possible by the generosity of Eric and Wendy Schmidt by recommendation of the Schmidt Futures program.

## Declarations

**Competing Interests** The authors declare that they have no competing interests. SHS is a guest editor of the Space Science Reviews topical collection "Strong Gravitational Lensing", which includes this review article.



## References

Amanullah R, Goobar A, Clément B, Cuby J-G, Dahle H, Dahlén T, Hjorth J, Fabbro S, Jönsson J, Kneib J-P, Lidman C, Limousin M, Milvang-Jensen B, Mörtsell E, Nordin J, Paech K, Richard J, Riehm T, Stanishev V, Watson D (2011) A highly magnified supernova at z = 1.703 behind the massive galaxy cluster A1689. Astrophys J Lett 742(1):7. https://doi.org/10.1088/2041-8205/742/1/L7

Amanullah R, Johansson J, Goobar A, Ferretti R, Papadogiannakis S, Petrushevska T, Brown PJ, Cao Y, Contreras C, Dahle H, Elias-Rosa N, Fynbo JPU, Gorosabel J, Guaita L, Hangard L, Howell DA, Hsiao EY, Kankare E, Kasliwal M, Leloudas G, Lundqvist P, Mattila S, Nugent P, Phillips MM, Sandberg A, Stanishev V, Sullivan M, Taddia F, Östlin G, Asadi S, Herrero-Illana R, Jensen JJ, Karhunen K, Lazarevic S, Varenius E, Santos P, Sridhar SS, Wallström SHJ, Wiegert J (2015) Diversity in extinction laws of type Ia supernovae measured between 0.2 and 2 $\mu$m. Mon Not R Astron Soc 453(3):3300–3328. https://doi.org/10.1093/mnras/stv1505

Auger MW, Treu T, Bolton AS, Gavazzi R, Koopmans LVE, Marshall PJ, Moustakas LA, Burles S (2010) The sloan lens ACS survey. X. Stellar, dynamical, and total mass correlations of massive early-type galaxies. Astrophys J 724(1):511–525. https://doi.org/10.1088/0004-637X/724/1/511

Bacon R, Accardo M, Adjali L, Anwand H, Bauer S, Biswas I, Blaizot J, Boudon D, Brau-Nogue S, Brinchmann J, Caillier P, Capoani L, Carollo CM, Contini T, Couderc P, Daguisé E, Deiries S, Delabre B, Dreizler S, Dubois J, Dupieux M, Dupuy C, Emsellem E, Fechner T, Fleischmann A, François M, Gallou G, Gharsa T, Glindemann A, Gojak D, Guiderdoni B, Hansali G, Hahn T, Jarno A, Kelz A, Koehler C, Kosmalski J, Laurent F, Le Floch M, Lilly SJ, Lizon J-L, Loupias M, Manescau A, Monstein C, Nicklas H, Olaya J-C, Pares L, Pasquini L, Pécontal-Rousset A, Pelló R, Petit C, Popow E, Reiss R, Remillieux A, Renault E, Roth M, Rupprecht G, Serre D, Schaye J, Soucail G, Steinmetz M, Streicher O, Stuik R, Valentin H, Vernet J, Weilbacher P, Wisotzki L, Yerle N (2010) The MUSE second-generation VLT instrument. In: McLean IS, Ramsay SK, Takami H (eds) Ground-based and airborne instrumentation for astronomy III. Society of photo-optical instrumentation engineers (SPIE) conference series, vol 7735, p 773508. https://doi.org/10.1117/12.856027

Bag S, Kim AG, Linder EV, Shafieloo A (2021) Be it unresolved: measuring time delays from lensed supernovae. Astrophys J 910(1):65. https://doi.org/10.3847/1538-4357/abe238

Bagherpour H, Branch D, Kantowski R (2006) Effects of gravitational microlensing on P Cygni profiles of type Ia supernovae. Astrophys J 638(2):946–950. https://doi.org/10.1086/498889

Barnabè M, Dutton AA, Marshall PJ, Auger MW, Brewer BJ, Treu T, Bolton AS, Koo DC, Koopmans LVE (2012) The SWELLS survey - IV. Precision measurements of the stellar and dark matter distributions in a spiral lens galaxy. Mon Not R Astron Soc 423(2):1073–1088. https://doi.org/10.1111/j.1365-2966.2012.20934.x

Bayer J, Huber S, Vogl C, Suyu SH, Taubenberger S, Sluse D, Chan JHH, Kerzendorf WE (2021) HOLISMOKES. V. Microlensing of type II supernovae and time-delay inference through spectroscopic phase retrieval. Astron Astrophys 653:A29. https://doi.org/10.1051/0004-6361/202040169. arXiv:2101.06229

Bellm EC, Kulkarni SR, Graham MJ, Dekany R, Smith RM, Riddle R, Masci FJ, Helou G, Prince TA, Adams SM, Barbarino C, Barlow T, Bauer J, Beck R, Belicki J, Biswas R, Blagorodnova N, Bodewits D, Bolin B, Brinnel V, Brooke T, Bue B, Bulla M, Burruss R, Cenko SB, Chang C-K, Connolly A, Coughlin M, Cromer J, Cunningham V, De K, Delacroix A, Desai V, Duev DA, Eadie G, Farnham TL, Feeney M, Feindt U, Flynn D, Franckowiak A, Frederick S, Fremling C, Gal-Yam A, Gezari S, Giomi M, Goldstein DA, Golkhou VZ, Goobar A, Groom S, Hacopians E, Hale D, Henning J, Ho AYQ, Hover D, Howell J, Hung T, Huppenkothen D, Imel D, Ip W-H, Ivezić Ž, Jackson E, Jones L, Juric M, Kasliwal MM, Kaspi S, Kaye S, Kelley MSP, Kowalski M, Kramer E, Kupfer T, Landry W, Laher RR, Lee C-D, Lin HW, Lin Z-Y, Lunnan R, Giomi M, Mahabal A, Mao P, Miller AA, Monkewitz S, Murphy P, Ngeow C-C, Nordin J, Nugent P, Ofek E, Patterson MT, Penprase B, Porter M, Rauch L, Rebbapragada U, Reiley D, Rigault M, Rodriguez H, van Roestel J, Rusholme B, van Santen J, Schulze S, Shupe DL, Singer LP, Soumagnac MT, Stein R, Surace J, Sollerman J, Szkody P, Taddia F, Terek S, Van Sistine A, van Velzen S, Vestrand WT, Walters R, Ward C, Ye Q-Z, Yu P-C, Yan L, Zolkower J (2019) The Zwicky Transient Facility: system overview, performance, and first results. Publ Astron Soc Pac 131(995):018002. https://doi.org/10.1088/1538-3873/aaecbe

Betoule M, Kessler R, Guy J, Mosher J, Hardin D, Biswas R, Astier P, El-Hage P, Konig M, Kuhlmann S, Marriner J, Pain R, Regnault N, Balland C, Bassett BA, Brown PJ, Campbell H, Carlberg RG, Cellier-Holzem F, Cinabro D, Conley A, D'Andrea CB, DePoy DL, doi M, Ellis RS, Fabbro S, Filippenko AV, Foley RJ, Frieman JA, Fouchez D, Galbany L, Goobar A, Gupta RR, Hill GJ, Hlozek R, Hogan CJ, Hook IM, Howell DA, Jha SW, Le Guillou L, Leloudas G, Lidman C, Marshall JL, Möller A, Mourão AM, Neveu J, Nichol R, Olmstead MD, Palanque-Delabrouille N, Perlmutter S, Prieto JL, Pritchet CJ, Richmond M, Riess AG, Ruhlmann-Kleider V, Sako M, Schahmaneche K, Schneider DP, Smith M, Sollerman J, Sullivan M, Walton NA, Wheeler CJ (2014) Improved cosmological constraints from a joint analysis of the SDSS-II and SNLS supernova samples. Astron Astrophys 568:22. https://doi.org/10.1051/0004-6361/201423413

Birrer S, Shajib AJ, Galan A, Millon M, Treu T, Agnello A, Auger M, Chen GC-F, Christensen L, Collett T, Courbin F, Fassnacht CD, Koopmans LVE, Marshall PJ, Park J-W, Rusu CE, Sluse D, Spiniello C, Suyu SH, Wagner-Carena S, Wong KC, Barnabè M, Bolton AS, Czoske O, Ding X, Frieman L, Van de Vyvere JA (2020) TDCOSMO. IV. Hierarchical time-delay cosmography – joint inference of the Hubble constant and galaxy density profiles. Astron Astrophys 643:165. https://doi.org/10.1051/0004-6361/202038861

Birrer S, Dhawan S, Shajib AJ (2022) The Hubble constant from strongly lensed supernovae with standardizable magnifications. Astrophys J 924:2. https://doi.org/10.3847/1538-4357/ac323a. arXiv:2107.12385

Birrer S, Millon M, Sluse D, Shajib AJ, Courbin F, Koopmans LVE, Suyu SH, Treu T (2024) Time-Delay Cosmography: Measuring the Hubble Constant and other cosmological parameters with strong gravitational lensing. Space Sci Rev 220. arXiv:2210.10833

Bloom JS, Kasen D, Shen KJ, Nugent PE, Butler NR, Graham ML, Howell DA, Kolb U, Holmes S, Haswell CA, Burwitz V, Rodriguez J, Sullivan M (2012) A compact degenerate primary-star progenitor of SN 2011fe. Astrophys J Lett 744(2):17. https://doi.org/10.1088/2041-8205/744/2/L17

Bolton AS, Burles S, Koopmans LVE, Treu T, Moustakas LA (2006) The Sloan Lens ACS survey. I. A large spectroscopically selected sample of massive early-type lens galaxies. Astrophys J 638(2):703–724. https://doi.org/10.1086/498884

Bolton AS, Burles S, Koopmans LVE, Treu T, Gavazzi R, Moustakas LA, Wayth R, Schlegel DJ (2008) The sloan lens ACS survey. V. The full ACS strong-lens sample. Astrophys J 682(2):964–984. https://doi.org/10.1086/589327

Bolton AS, Brownstein JR, Kochanek CS, Shu Y, Schlegel DJ, Eisenstein DJ, Wake DA, Connolly N, Maraston C, Arneson RA, Weaver BA (2012) The BOSS emission-line lens survey. II. Investigating mass-density profile evolution in the SLACS+BELLS strong gravitational lens sample. Astrophys J 757(1):82. https://doi.org/10.1088/0004-637X/757/1/82

Brownstein JR, Bolton AS, Schlegel DJ, Eisenstein DJ, Kochanek CS, Connolly N, Maraston C, Pandey P, Seitz S, Wake DA, Wood-Vasey WM, Brinkmann J, Schneider DP, Weaver BA (2012) The BOSS emission-line lens survey (BELLS). I. A large spectroscopically selected sample of lens galaxies at redshift ∼0.5. Astrophys J 744(1):41. https://doi.org/10.1088/0004-637X/744/1/41

Bulla M, Miller AA, Yao Y, Dessart L, Dhawan S, Papadogiannakis S, Biswas R, Goobar A, Kulkarni SR, Nordin J, Nugent P, Polin A, Sollerman J, Bellm EC, Coughlin MW, Dekany R, Golkhou VZ, Graham MJ, Kasliwal MM, Kupfer T, Laher RR, Masci FJ, Porter M, Rusholme B, Shupe DL (2020) ZTF Early Observations of Type Ia Supernovae III: Early-Time Colors as a Test for Explosion Models and Multiple Populations. Astrophys J 902:48. https://doi.org/10.3847/1538-4357/abb13c. arXiv:2001.00587

Cañameras R, Nesvadba NPH, Guery D, McKenzie T, König S, Petitpas G, Dole H, Frye B, Flores-Cacho I, Montier L, Negrello M, Beelen A, Boone F, Dicken D, Lagache G, Le Floc'h E, Altieri B, Béthermin M, Chary R, de Zotti G, Giard M, Kneissl R, Krips M, Malhotra S, Martinache C, Omont A, Pointecouteau E, Puget J-L, Scott D, Soucail G, Valtchanov I, Welikala N, Yan L (2015) Planck's dusty GEMS: the brightest gravitationally lensed galaxies discovered with the Planck all-sky survey. Astron Astrophys 581:105. https://doi.org/10.1051/0004-6361/201425128

Cañameras R, Nesvadba NPH, Limousin M, Dole H, Kneissl R, Koenig S, Le Floc'h E, Petitpas G, Scott D (2018) Planck's dusty GEMS. V. Molecular wind and clump stability in a strongly lensed star-forming galaxy at z = 2.2. Astron Astrophys 620:60. https://doi.org/10.1051/0004-6361/201833679

Cañameras R, Schuldt S, Suyu SH, Taubenberger S, Meinhardt T, Leal-Taixé L, Lemon C, Rojas K, Savary E (2020) HOLISMOKES. II. Identifying galaxy-scale strong gravitational lenses in Pan-STARRS using convolutional neural networks. Astron Astrophys 644:163. https://doi.org/10.1051/0004-6361/202038219

Cañameras R, Schuldt S, Shu Y, Suyu SH, Taubenberger S, Meinhardt T, Leal-Taixé L, Chao DC-Y, Inoue KT, Jaelani AT, More A (2021) HOLISMOKES. VI. New galaxy-scale strong lens candidates from the HSC-SSP imaging survey. Astron Astrophys 653:L6. https://doi.org/10.1051/0004-6361/202141758. arXiv:2107.07829

Chen W, Kelly PL, Oguri M, Broadhurst TJ, Diego JM, Emami N, Filippenko AV, Treu TL, Zitrin A (2022) Shock cooling of a red-supergiant supernova at redshift 3 in lensed images. Nature 611(7935):256–259. https://doi.org/10.1038/s41586-022-05252-5

Chirivì G, Yıldırım A, Suyu SH, Halkola A (2020) Gravitational lensing and dynamics (GLaD): combined analysis to unveil properties of high-redshift galaxies. Astron Astrophys 643:135. https://doi.org/10.1051/0004-6361/202037929

Chornock R, Berger E, Rest A, Milisavljevic D, Lunnan R, Foley RJ, Soderberg AM, Smartt SJ, Burgasser AJ, Challis P, Chomiuk L, Czekala I, Drout M, Fong W, Huber ME, Kirshner RP, Leibler C, McLeod B, Marion GH, Narayan G, Riess AG, Roth KC, Sanders NE, Scolnic D, Smith K, Stubbs CW, Tonry JL, Valenti S, Burgett WS, Chambers KC, Hodapp KW, Kaiser N, Kudritzki R-P, Magnier EA, Price PA (2013) PS1-10afx at z = 1.388: Pan-STARRS1 discovery of a new type of superluminous supernova. Astrophys J 767(2):162. https://doi.org/10.1088/0004-637X/767/2/162

Courbin F, Bonvin V, Buckley-Geer E, Fassnacht CD, Frieman J, Lin H, Marshall PJ, Suyu SH, Treu T, Anguita T, Motta V, Meylan G, Paic E, Tewes M, Agnello A, Chao DC-Y, Chijani M, Gilman D, Rojas K, Williams P, Hempel A, Kim S, Lachaume R, Rabus M, Abbott TMC, Allam S, Annis J, Banerji M, Bechtol K, Benoit-Lévy A, Brooks D, Burke DL, Carnero Rosell A, Carrasco Kind M, Carretero J, D'Andrea CB, da Costa LN, Davis C, DePoy DL, Desai S, Flaugher B, Fosalba P, García-Bellido J, Gaztanaga E, Goldstein DA, Gruen D, Gruendl RA, Gschwend J, Gutierrez G, Honscheid K, James DJ, Kuehn K, Kuhlmann S, Kuropatkin N, Lahav O, Lima M, Maia MAG, March M, Marshall JL, McMahon RG, Menanteau F, Miquel R, Nord B, Plazas AA, Sanchez E, Scarpine V, Schindler R, Schubnell M, Sevilla-Noarbe I, Smith M, Soares-Santos M, Sobreira F, Suchyta E, Tarle G, Tucker DL, Walker AR, Wester W (2018) COSMOGRAIL: the COSmological MOnitoring of GRAvItational lenses. XVI. Time delays for the quadruply imaged quasar DES J0408-5354 with high-cadence photometric monitoring. Astron Astrophys 609:71. https://doi.org/10.1051/0004-6361/201731461

Craig P, O'Connor K, Chakrabarti S, Rodney SA, Pierel JR, McCully C, Perez-Fournon I (2021) A targeted search for strongly lensed supernovae and expectations for targeted searches in the Rubin era. ArXiv e-prints, arXiv:2111.01680

Denissenya M, Linder EV (2022) Deep learning unresolved lensed light curves. Mon Not R Astron Soc 515(1):977–983. https://doi.org/10.1093/mnras/stac1726

Dhawan S, Johansson J, Goobar A, Amanullah R, Mörtsell E, Cenko SB, Cooray A, Fox O, Goldstein D, Kalender R, Kasliwal M, Kulkarni SR, Lee WH, Nayyeri H, Nugent P, Ofek E, Quimby R (2020) Magnification, dust, and time-delay constraints from the first resolved strongly lensed type Ia supernova iPTF16geu. Mon Not R Astron Soc 491(2):2639–2654. https://doi.org/10.1093/mnras/stz2965

Di Valentino E, Mena O, Pan S, Visinelli L, Yang W, Melchiorri A, Mota DF, Riess AG, Silk J (2021) In the realm of the Hubble tension-a review of solutions. Class Quantum Gravity 38(15):153001. https://doi.org/10.1088/1361-6382/ac086d

Diego JM, Bernstein G, Chen W, Goobar A, Johansson JP, Kelly PL, Mörtsell E, Nightingale JW (2022) Microlensing and the type Ia supernova iPTF16geu. Astron Astrophys 662:34. https://doi.org/10.1051/0004-6361/202143009

Ding X, Liao K, Birrer S, Shajib AJ, Treu T, Yang L (2021) Improved time-delay lens modelling and $H_0$ inference with transient sources. Mon Not R Astron Soc 504(4):5621–5628. https://doi.org/10.1093/mnras/stab1240

Dobler G, Keeton CR (2006) Microlensing of lensed supernovae. Astrophys J 653(2):1391–1399. https://doi.org/10.1086/508769

Einstein A (1936) Lens-like action of a star by the deviation of light in the gravitational field. Science 84(2188):506–507. https://doi.org/10.1126/science.84.2188.506

Elíasdóttir Á, Hjorth J, Toft S, Burud I, Paraficz D (2006) Extinction curves of lensing galaxies out to z = 1. Astrophys J Suppl Ser 166(2):443–469. https://doi.org/10.1086/507131

Falco EE, Gorenstein MV, Shapiro II (1985) On model-dependent bounds on H 0 from gravitational images: application to Q 0957+561 A, B. Astrophys J Lett 289:1–4. https://doi.org/10.1086/184422

Falco EE, Impey CD, Kochanek CS, Lehár J, McLeod BA, Rix H-W, Keeton CR, Muñoz JA, Peng CY (1999) Dust and extinction curves in galaxies with z>0: the interstellar medium of gravitational lens galaxies. Astrophys J 523(2):617–632. https://doi.org/10.1086/307758

Fassnacht CD, Xanthopoulos E, Koopmans LVE, Rusin D (2002) A determination of $H_0$ with the CLASS gravitational lens B1608+656. III. A significant improvement in the precision of the time delay measurements. Astrophys J 581(2):823–835. https://doi.org/10.1086/344368

Fausnaugh MM, Vallely PJ, Kochanek CS, Shappee BJ, Stanek KZ, Tucker MA, Ricker GR, Vanderspek R, Latham DW, Seager S, Winn JN, Jenkins JM, Daylan T, Doty JP, Furesz G, Levine AM, Morris R, Pal A, Sha L, Ting EB, Wohler B (2021) Early-time light curves of type Ia supernovae observed with TESS. Astrophys J 908:51. https://doi.org/10.3847/1538-4357/abcd42. arXiv:1904.02171

Fink M, Hillebrandt W, Röpke FK (2007) Double-detonation supernovae of sub-Chandrasekhar mass white dwarfs. Astron Astrophys 476(3):1133–1143. https://doi.org/10.1051/0004-6361:20078438

Fitzpatrick EL, Massa D (2007) An analysis of the shapes of interstellar extinction curves. V. The IR-through-UV curve morphology. Astrophys J 663(1):320–341. https://doi.org/10.1086/518158

Foxley-Marrable M, Collett TE, Vernardos G, Goldstein DA, Bacon D (2018) The impact of microlensing on the standardization of strongly lensed type Ia supernovae. Mon Not R Astron Soc 478(4):5081–5090. https://doi.org/10.1093/mnras/sty1346

Foxley-Marrable M, Collett TE, Frohmaier C, Goldstein DA, Kasen D, Swann E, Bacon D (2020) Observing the earliest moments of supernovae using strong gravitational lenses. Mon Not R Astron Soc 495(4):4622–4637. https://doi.org/10.1093/mnras/staa1289

Frye BL, Pascale M, Qin Y, Zitrin A, Diego J, Walth G, Yan H, Conselice CJ, Alpaslan M, Bauer A, Busoni L, Coe D, Cohen SH, Dole H, Donahue M, Georgiev I, Jansen RA, Limousin M, Livermore R, Norman D, Rabien S, Windhorst RA (2019) analysis of a massive lensing cluster in a Hubble space telescope census of submillimeter giant arcs selected using Planck/Herschel. Astrophys J 871(1):51. https://doi.org/10.3847/1538-4357/aaeff7

Frye BL, Pascale M, Pierel J, Chen W, Foo N, Leimbach R, Garuda N, Cohen S, Kamieneski P, Windhorst R, Koekemoer AM, Kelly P, Summers J, Engesser M, Liu D, Furtak L, Polletta M, Harrington K, Willner S, Diego JM, Jansen R, Coe D, Conselice CJ, Dai L, Dole H, D'Silva JCJ, Driver S, Grogin N, Marshall MA, Meena A, Nonino M, Ortiz Rafael I, Pirzkal N, Robotham A, Ryan RE, Strolger L, Tompkins S, Trussler J, Willmer C, Yan H, Yun MS, Zitrin A (2023) The JWST Discovery of the Triply-imaged Type Ia "Supernova H0pe" and Observations of the Galaxy Cluster PLCK G165.7+67.0. ArXiv e-prints, arXiv:2309.07326

Gavazzi R, Treu T, Marshall PJ, Brault F, Ruff A (2012) The SL2S galaxy-scale gravitational lens sample. I. The alignment of mass and light in massive early-type galaxies at z = 0.2-0.9. Astrophys J 761(2):170. https://doi.org/10.1088/0004-637X/761/2/170

Goldstein DA, Nugent PE (2017) How to find gravitationally lensed type Ia supernovae. Astrophys J Lett 834(1):5. https://doi.org/10.3847/2041-8213/834/1/L5

Goldstein DA, Nugent PE, Kasen DN, Collett TE (2018) Precise time delays from strongly gravitationally lensed type Ia supernovae with chromatically microlensed images. Astrophys J 855(1):22. https://doi.org/10.3847/1538-4357/aaa975

Goldstein DA, Nugent PE, Goobar A (2019) Rates and properties of supernovae strongly gravitationally lensed by elliptical galaxies in time-domain imaging surveys. Astrophys J Suppl Ser 243(1):6 https://doi.org/10.3847/1538-4365/ab1fe0

González Hernández JI, Ruiz-Lapuente P, Tabernero HM, Montes D, Canal R, Méndez J, Bedin LR (2012) No surviving evolved companions of the progenitor of SN 1006. Nature 489(7417):533–536. https://doi.org/10.1038/nature11447

González-Gaitán S, Tominaga N, Molina J, Galbany L, Bufano F, Anderson JP, Gutierrez C, Förster F, Pignata G, Bersten M, Howell DA, Sullivan M, Carlberg R, de Jaeger T, Hamuy M, Baklanov PV, Blinnikov SI (2015) The rise-time of type II supernovae. Mon Not R Astron Soc 451(2):2212–2229. https://doi.org/10.1093/mnras/stv1097

Goobar A, Mörtsell E, Amanullah R, Nugent P (2002) Cosmological parameters from lensed supernovae. Astron Astrophys 393:25–32. https://doi.org/10.1051/0004-6361:20020987

Goobar A, Paech K, Stanishev V, Amanullah R, Dahlén T, Jönsson J, Kneib JP, Lidman C, Limousin M, Mörtsell E, Nobili S, Richard J, Riehm T, von Strauss M (2009) Near-IR search for lensed supernovae behind galaxy clusters. II. First detection and future prospects. Astron Astrophys 507(1):71–83. https://doi.org/10.1051/0004-6361/200811254

Goobar A, Kromer M, Siverd R, Stassun KG, Pepper J, Amanullah R, Kasliwal M, Sollerman J, Taddia F (2015) Constraints on the origin of the first light from SN 2014J. Astrophys J 799(1):106. https://doi.org/10.1088/0004-637X/799/1/106

Goobar A, Amanullah R, Kulkarni SR, Nugent PE, Johansson J, Steidel C, Law D, Mörtsell E, Quimby R, Blagorodnova N, Brandeker A, Cao Y, Cooray A, Ferretti R, Fremling C, Hangard L, Kasliwal M, Kupfer T, Lunnan R, Masci F, Miller AA, Nayyeri H, Neill JD, Ofek EO, Papadogiannakis S, Petrushevska T, Ravi V, Sollerman J, Sullivan M, Taddia F, Walters R, Wilson D, Yan L, Yaron O (2017) IPTF16geu: a multiply imaged, gravitationally lensed type Ia supernova. Science 356(6335):291–295. https://doi.org/10.1126/science.aal2729

Goobar A, Johansson J, Schulze S, Arendse N, Sagués Carracedo A, Dhawan S, Mörtsell E, Fremling C, Yan L, Perley D, Sollerman J, Joseph R, Hinds K-R, Meynardie W, Andreoni I, Bellm E, Bloom J, Collett TE, Drake A, Graham M, Kasliwal M, Kulkarni S, Miller A, Neill JD, Nordin J, Pierel J, Richard J, Riddle R, Rigault M, Rusholme B, Sharma Y, Stein R, Stewart G, Townsend A, Vinko J, Wheeler JC, Wold A (2023) SN Zwicky: uncovering a population of gravitational lens galaxies with magnified "standard candles". Nat Astron 7:1098–1107. https://doi.org/10.1038/s41550-023-01981-3. arXiv:2211.00656

Grillo C, Karman W, Suyu SH, Rosati P, Balestra I, Mercurio A, Lombardi M, Treu T, Caminha GB, Halkola A, Rodney SA, Gavazzi R, Caputi KI (2016) The story of supernova "refsdal" told by muse. Astrophys J 822(2):78. https://doi.org/10.3847/0004-637X/822/2/78

Grillo C, Rosati P, Suyu SH, Balestra I, Caminha GB, Halkola A, Kelly PL, Lombardi M, Mercurio A, Rodney SA, Treu T (2018) Measuring the value of the Hubble constant "à la Refsdal". Astrophys J 860(2):94. https://doi.org/10.3847/1538-4357/aac2c9

Grillo C, Rosati P, Suyu SH, Caminha GB, Mercurio A, Halkola A (2020) On the accuracy of time-delay cosmography in the frontier fields cluster MACS J1149.5+2223 with supernova Refsdal. Astrophys J 898(1):87. https://doi.org/10.3847/1538-4357/ab9a4c

Gunnarsson C, Goobar A (2003) Massive galaxy clusters as gravitational telescopes for distant supernovae. Astron Astrophys 405:859–866. https://doi.org/10.1051/0004-6361:20030648

Harrington KC, Yun MS, Cybulski R, Wilson GW, Aretxaga I, Chavez M, De la Luz V, Erickson N, Ferrusca D, Gallup AD, Hughes DH, Montaña A, Narayanan G, Sánchez-Argüelles D, Schloerb FP, Souccar K, Terlevich E, Terlevich R, Zeballos M, Zavala JA (2016) Early science with the large millimeter telescope: observations of extremely luminous high-z sources identified by Planck. Mon Not R Astron Soc 458(4):4383–4399. https://doi.org/10.1093/mnras/stw614

Hjorth J, Vreeswijk PM, Gall C, Watson D (2013) On inferring extinction laws in z $\sim$ 6 quasars as signatures of supernova dust. Astrophys J 768(2):173. https://doi.org/10.1088/0004-637X/768/2/173

Huang X, Storfer C, Ravi V, Pilon A, Domingo M, Schlegel DJ, Bailey S, Dey A, Gupta RR, Herrera D, Juneau S, Landriau M, Lang D, Meisner A, Moustakas J, Myers AD, Schlafly EF, Valdes F, Weaver BA, Yang J, Yèche C (2020) Finding strong gravitational lenses in the DESI DECam legacy survey. Astrophys J 894(1):78. https://doi.org/10.3847/1538-4357/ab7ffb

Huang X, Storfer C, Gu A, Ravi V, Pilon A, Sheu W, Venguswamy R, Banka S, Dey A, Landriau M, Lang D, Meisner A, Moustakas J, Myers AD, Sajith R, Schlafly EF, Schlegel DJ (2021) Discovering new strong gravitational lenses in the DESI legacy imaging surveys. Astrophys J 909(1):27. https://doi.org/10.3847/1538-4357/abd62b

Huber S, Suyu SH, Noebauer UM, Bonvin V, Rothchild D, Chan JHH, Awan H, Courbin F, Kromer M, Marshall P, Oguri M, Ribeiro T, LSST dark energy science collaboration (2019) Strongly lensed SNe Ia in the era of LSST: observing cadence for lens discoveries and time-delay measurements. Astron Astrophys 631:161. https://doi.org/10.1051/0004-6361/201935370

Huber S, Suyu SH, Ghoshdastidar D, Taubenberger S, Bonvin V, Chan JHH, Kromer M, Noebauer UM, Sim SA, Leal-Taixé L (2021a) HOLISMOKES. VII. Time-delay measurement of strongly lensed SNe Ia using machine learning. Astron Astrophys 658:A157. https://doi.org/10.1051/0004-6361/202141956. arXiv:2108.02789

Huber S, Suyu SH, Noebauer UM, Chan JHH, Kromer M, Sim SA, Sluse D, Taubenberger S (2021b) HOLISMOKES. III. Achromatic phase of strongly lensed type Ia supernovae. Astron Astrophys 646:110. https://doi.org/10.1051/0004-6361/202039218

Iben I Jr, Tutukov AV (1984) Supernovae of type I as end products of the evolution of binaries with components of moderate initial mass ($M \lesssim 9\ M_{\odot}$). Astrophys J Suppl Ser 54:335–372. https://doi.org/10.1086/190932

Jacobs C, Glazebrook K, Collett T, More A, McCarthy C (2017) Finding strong lenses in CFHTLS using convolutional neural networks. Mon Not R Astron Soc 471(1):167–181. https://doi.org/10.1093/mnras/stx1492

Jacobs C, Collett T, Glazebrook K, Buckley-Geer E, Diehl HT, Lin H, McCarthy C, Qin AK, Odden C, Caso Escudero M, Dial P, Yung VJ, Gaitsch S, Pellico A, Lindgren KA, Abbott TMC, Annis J, Avila S, Brooks D, Burke DL, Carnero Rosell A, Carrasco Kind M, Carretero J, da Costa LN, De Vicente J, Fosalba P, Frieman J, García-Bellido J, Gaztanaga E, Goldstein DA, Gruen D, Gruendl RA, Gschwend J, Hollowood DL, Honscheid K, Hoyle B, James DJ, Krause E, Kuropatkin N, Lahav O, Lima M, Maia MAG, Marshall JL, Miquel R, Plazas AA, Roodman A, Sanchez E, Scarpine V, Serrano S, Sevilla-Noarbe I, Smith M, Sobreira F, Suchyta E, Swanson MEC, Tarle G, Vikram V, Walker AR, Zhang Y, DES Collaboration (2019) An extended catalog of galaxy-galaxy strong gravitational lenses discovered in DES using convolutional neural networks. Astrophys J Suppl Ser 243(1):17. https://doi.org/10.3847/1538-4365/ab26b6

Jauzac M, Richard J, Limousin M, Knowles K, Mahler G, Smith GP, Kneib J-P, Jullo E, Natarajan P, Ebeling H, Atek H, Clément B, Eckert D, Egami E, Massey R, Rexroth M (2016) Hubble frontier fields: predictions for the return of SN Refsdal with the MUSE and GMOS spectrographs. Mon Not R Astron Soc 457(2):2029–2042. https://doi.org/10.1093/mnras/stw069

Jee I, Komatsu E, Suyu SH (2015) Measuring angular diameter distances of strong gravitational lenses. J Cosmol Astropart Phys 2015(11):033. https://doi.org/10.1088/1475-7516/2015/11/033

Jee I, Komatsu E, Suyu SH, Huterer D (2016) Time-delay cosmography: increased leverage with angular diameter distances. J Cosmol Astropart Phys 2016(4):031. https://doi.org/10.1088/1475-7516/2016/04/031

Jee I, Suyu SH, Komatsu E, Fassnacht CD, Hilbert S, Koopmans LVE (2019) A measurement of the Hubble constant from angular diameter distances to two gravitational lenses. Science 365(6458):1134–1138. https://doi.org/10.1126/science.aat7371

Johansson J, Goobar A, Price SH, Sagués Carracedo A, Della Bruna L, Nugent PE, Dhawan S, Mörtsell E, Papadogiannakis S, Amanullah R, Goldstein D, Cenko SB, De K, Dugas A, Kasliwal MM, Kulkarni SR, Lunnan R (2021) Spectroscopy of the first resolved strongly lensed type Ia supernova iPTF16geu. Mon Not R Astron Soc 502(1):510–520. https://doi.org/10.1093/mnras/staa3829

Jones DO, Foley RJ, Narayan G, Hjorth J, Huber ME, Aleo PD, Alexander KD, Angus CR, Auchettl K, Baldassare VF, Bruun SH, Chambers KC, Chatterjee D, Coppejans DL, Coulter DA, DeMarchi L, Dimitriadis G, Drout MR, Engel A, French KD, Gagliano A, Gall C, Hung T, Izzo L, Jacobson-Galán WV, Kilpatrick CD, Korhonen H, Margutti R, Raimundo SI, Ramirez-Ruiz E, Rest A, Rojas-Bravo C, Siebert MR, Smartt SJ, Smith KW, Terreran G, Wang Q, Wojtak R, Agnello A, Ansari Z, Arendse N, Baldeschi A, Blanchard PK, Brethauer D, Bright JS, Brown JS, de Boer TJL, Dodd SA, Fairlamb JR, Grillo C, Hajela A, Hede C, Kolborg AN, Law-Smith JAP, Lin C-C, Magnier EA, Malanchev K, Matthews D, Mockler B, Muthukrishna D, Pan Y-C, Pfister H, Ramanah DK, Rest S, Sarangi A, Schrøder SL, Stauffer C, Stroh MC, Taggart KL, Tinyanont S, Wainscoat RJ (2021) young supernova experiment, the young supernova experiment: survey goals, overview, and operations. Astrophys J 908(2):143. https://doi.org/10.3847/1538-4357/abd7f5

Kasen D (2010) Seeing the collision of a supernova with its companion star. Astrophys J 708(2):1025–1031. https://doi.org/10.1088/0004-637X/708/2/1025

Kawamata R, Oguri M, Ishigaki M, Shimasaku K, Ouchi M (2016) Precise strong lensing mass modeling of four Hubble frontier field clusters and a sample of magnified high-redshift galaxies. Astrophys J 819(2):114. https://doi.org/10.3847/0004-637X/819/2/114

Kelly PL, Rodney SA, Treu T, Foley RJ, Brammer G, Schmidt KB, Zitrin A, Sonnenfeld A, Strolger L-G, Graur O, Filippenko AV, Jha SW, Riess AG, Bradac M, Weiner BJ, Scolnic D, Malkan MA, von der Linden A, Trenti M, Hjorth J, Gavazzi R, Fontana A, Merten JC, McCully C, Jones T, Postman M, Dressler A, Patel B, Cenko SB, Graham ML, Tucker BE (2015) Multiple images of a highly magnified supernova formed by an early-type cluster galaxy lens. Science 347(6226):1123–1126. https://doi.org/10.1126/science.aaa3350

Kelly PL, Brammer G, Selsing J, Foley RJ, Hjorth J, Rodney SA, Christensen L, Strolger L-G, Filippenko AV, Treu T, Steidel CC, Strom A, Riess AG, Zitrin A, Schmidt KB, Bradač M, Jha SW, Graham ML, McCully C, Graur O, Weiner BJ, Silverman JM, Taddia F (2016b) SN Refsdal: classification as a luminous and blue SN 1987A-like type II supernova. Astrophys J 831(2):205. https://doi.org/10.3847/0004-637X/831/2/205

Kelly PL, Rodney SA, Treu T, Strolger L-G, Foley RJ, Jha SW, Selsing J, Brammer G, Bradač M, Cenko SB, Graur O, Filippenko AV, Hjorth J, McCully C, Molino A, Nonino M, Riess AG, Schmidt KB, Tucker B,

von der Linden A, Weiner BJ, Zitrin A (2016a) Deja vu all over again: the reappearance of supernova Refsdal. Astrophys J Lett 819(1):8. https://doi.org/10.3847/2041-8205/819/1/L8

Kelly PL, Rodney S, Treu T, Birrer S, Bonvin V, Dessart L, Foley RJ, Filippenko AV, Gilman D, Jha S, Hjorth J, Mandel K, Millon M, Pierel J, Thorp S, Zitrin A, Broadhurst T, Chen W, Diego JM, Dressler A, Graur O, Jauzac M, Malkan MA, McCully C, Oguri M, Postman M, Schmidt KB, Sharon K, Tucker BE, von der Linden A, Wambsganss J (2023b) The magnificent five images of supernova Refsdal: time delay and magnification measurements. Astrophys J 948(2):93. https://doi.org/10.3847/1538-4357/ac4ccb

Kelly PL, Rodney S, Treu T, Oguri M, Chen W, Zitrin A, Birrer S, Bonvin V, Dessart L, Diego JM, Filippenko AV, Foley RJ, Gilman D, Hjorth J, Jauzac M, Mandel K, Millon M, Pierel J, Sharon K, Thorp S, Williams L, Broadhurst T, Dressler A, Graur O, Jha S, McCully C, Postman M, Schmidt KB, Tucker BE, von der Linden A (2023a) Constraints on the Hubble constant from supernova Refsdal's reappearance. Science 380(6649):1322. https://doi.org/10.1126/science.abh1322

Kerzendorf WE, Sim SA (2014) A spectral synthesis code for rapid modelling of supernovae. Mon Not R Astron Soc 440(1):387–404. https://doi.org/10.1093/mnras/stu055

Kochanek CS (2019) The physics of flash (supernova) spectroscopy. Mon Not R Astron Soc 483(3):3762–3772. https://doi.org/10.1093/mnras/sty3363

Kodi Ramanah D, Arendse N, Wojtak R (2022) AI-driven spatio-temporal engine for finding gravitationally lensed supernovae. Mon Not R Astron Soc 512(4):5404–5417. https://doi.org/10.1093/mnras/stac838. arXiv:2107.12399

Kolatt TS, Bartelmann M (1998) Gravitational lensing of type IA supernovae by galaxy clusters. Mon Not R Astron Soc 296(3):763–772. https://doi.org/10.1046/j.1365-8711.1998.01466.x

Kovner I, Paczynski B (1988) Supernovae in luminous arcs. Astrophys J Lett 335:9. https://doi.org/10.1086/185328

Lanusse F, Ma Q, Li N, Collett TE, Li C-L, Ravanbakhsh S, Mandelbaum R, Póczos B (2018) CMU DeepLens: deep learning for automatic image-based galaxy-galaxy strong lens finding. Mon Not R Astron Soc 473(3):3895–3906. https://doi.org/10.1093/mnras/stx1665

Lee C-H, Matheson T, Saha A, Narayan G, Soraisam M, Stubens C, Wolf N, Snodgrass R, Kececioglu J, Scheidegger C (2020) ANTARES: a gateway to ZTF and LSST alerts. In: Society of photo-optical instrumentation engineers (SPIE) conference series, vol 11449. https://doi.org/10.1117/12.2560698

Liao K, Biesiada M, Zhu Z-H (2022) Strongly lensed transient sources: a review. Chin Phys Lett 39(11):119801. https://doi.org/10.1088/0256-307X/39/11/119801

Limousin M, Cabanac R, Gavazzi R, Kneib J-P, Motta V, Richard J, Thanjavur K, Foex G, Pello R, Crampton D, Faure C, Fort B, Jullo E, Marshall P, Mellier Y, More A, Soucail G, Suyu S, Swinbank M, Sygnet J-F, Tu H, Valls-Gabaud D, Verdugo T, Willis J (2009) A new window of exploration in the mass spectrum: strong lensing by galaxy groups in the SL2S. Astron Astrophys 502(2):445–456. https://doi.org/10.1051/0004-6361/200811473

Livio M, Mazzali P (2018) On the progenitors of type Ia supernovae. Phys Rep 736:1–23. https://doi.org/10.1016/j.physrep.2018.02.002

LSST Science Collaboration, Abell PA, Allison J, Anderson SF, Andrew JR, Angel JRP, Armus L, Arnett D, Asztalos SJ, Axelrod TS, Bailey S, Ballantyne DR, Bankert JR, Barkhouse WA, Barr JD, Barrientos LF, Barth AJ, Bartlett JG, Becker AC, Becla J, Beers TC, Bernstein JP, Biswas R, Blanton MR, Bloom JS, Bochanski JJ, Boeshaar P, Borne KD, Bradac M, Brandt WN, Bridge CR, Brown ME, Brunner RJ, Bullock JS, Burgasser AJ, Burge JH, Burke DL, Cargile PA, Chandrasekharan S, Chartas G, Chesley SR, Chu Y-H, Cinabro D, Claire MW, Claver CF, Clowe D, Connolly AJ, Cook KH, Cooke J, Cooray A, Covey KR, Culliton CS, de Jong R, de Vries WH, Debattista VP, Delgado F, Dell'Antonio IP, Dhital S, Di Stefano R, Dickinson M, Dilday B, Djorgovski SG, Dobler G, Donalek C, Dubois-Felsmann G, Durech J, Eliasdottir A, Eracleous M, Eyer L, Falco EE, Fan X, Fassnacht CD, Ferguson HC, Fernandez YR, Fields BD, Finkbeiner D, Figueroa EE, Fox DB, Francke H, Frank JS, Frieman J, Fromenteau S, Furqan M, Galaz G, Gal-Yam A, Garnavich P, Gawiser E, Geary J, Gee P, Gibson RR, Gilmore K, Grace EA, Green RF, Gressler WJ, Grillmair CJ, Habib S, Haggerty JS, Hamuy M, Harris AW, Hawley SL, Heavens AF, Hebb L, Henry TJ, Hileman E, Hilton EJ, Hoadley K, Holberg JB, Holman MJ, Howell SB, Infante L, Ivezic Z, Jacoby SH, Jain B, Jedicke R, Jee MJ, Garrett Jernigan J, Jha SW, Johnston KV, Jones RL, Juric M, Kaasalainen S, Kafka M (2009) LSST Science Book, Version 2.0. ArXiv e-prints, arXiv:0912.0201

Lundqvist P, Nyholm A, Taddia F, Sollerman J, Johansson J, Kozma C, Lundqvist N, Fransson C, Garnavich PM, Kromer M, Shappee BJ, Goobar A (2015) No trace of a single-degenerate companion in late spectra of supernovae 2011fe and 2014J. Astron Astrophys 577:39. https://doi.org/10.1051/0004-6361/201525719

Maoz D, Mannucci F, Nelemans G (2014) Observational clues to the progenitors of type Ia supernovae. Annu Rev Astron Astrophys 52:107–170. https://doi.org/10.1146/annurev-astro-082812-141031

Marshall PJ, Verma A, More A, Davis CP, More S, Kapadia A, Parrish M, Snyder C, Wilcox J, Baeten E, Macmillan C, Cornen C, Baumer M, Simpson E, Lintott CJ, Miller D, Paget E, Simpson R, Smith AM, Küng R, Saha P, Collett TE (2016) SPACE WARPS - I. Crowdsourcing the discovery of gravitational lenses. Mon Not R Astron Soc 455(2):1171–1190. https://doi.org/10.1093/mnras/stv2009

Matheson T, Stubens C, Wolf N, Lee C-H, Narayan G, Saha A, Scott A, Soraisam M, Bolton AS, Hauger B, Silva DR, Kececioglu J, Scheidegger C, Snodgrass R, Aleo PD, Evans-Jacquez E, Singh N, Wang Z, Yang S, Zhao Z (2021) The ANTARES astronomical time-domain event broker. Astron J 161(3):107. https://doi.org/10.3847/1538-3881/abd703

Metcalf RB, Meneghetti M, Avestruz C, Bellagamba F, Bom CR, Bertin E, Cabanac R, Courbin F, Davies A, Decencière E, Flamary R, Gavazzi R, Geiger M, Hartley P, Huertas-Company M, Jackson N, Jacobs C, Jullo E, Kneib J-P, Koopmans LVE, Lanusse F, Li C-L, Ma Q, Makler M, Li N, Lightman M, Petrillo CE, Serjeant S, Schäfer C, Sonnenfeld A, Tagore A, Tortora C, Tuccillo D, Valentín MB, Velasco-Forero S, Verdoes Kleijn GA, Vernardos G (2019) The strong gravitational lens finding challenge. Astron Astrophys 625:119. https://doi.org/10.1051/0004-6361/201832797

Miller AA, Kasliwal MM, Cao Y, Adams SM, Goobar A, Knežević S, Laher RR, Lunnan R, Masci FJ, Nugent PE, Perley DA, Petrushevska T, Quimby RM, Rebbapragada UD, Sollerman J, Taddia F, Kulkarni SR (2017) Color me intrigued: the discovery of iPTF 16fnm, an SN 2002cx-like object. Astrophys J 848(1):59. https://doi.org/10.3847/1538-4357/aa8c7e

Miller AA, Yao Y, Bulla M, Pankow C, Bellm EC, Cenko SB, Dekany R, Fremling C, Graham MJ, Kupfer T, Laher RR, Mahabal AA, Masci FJ, Nugent PE, Riddle R, Rusholme B, Smith RM, Shupe DL, van Roestel J, Kulkarni SR (2020) ZTF Early Observations of Type Ia Supernovae II: First Light, the Initial Rise, and Time to Reach Maximum Brightness. Astrophys J 902:47. https://doi.org/10.3847/1538-4357/abb13b. arXiv:2001.00598

Millon M, Courbin F, Bonvin V, Buckley-Geer E, Fassnacht CD, Frieman J, Marshall PJ, Suyu SH, Treu T, Anguita T, Motta V, Agnello A, Chan JHH, Chao DC-Y, Chijani M, Gilman D, Gilmore K, Lemon C, Lucey JR, Melo A, Paic E, Rojas K, Sluse D, Williams PR, Hempel A, Kim S, Lachaume R, Rabus M (2020b) TDCOSMO. II. Six new time delays in lensed quasars from high-cadence monitoring at the MPIA 2.2 m telescope. Astron Astrophys 642:193. https://doi.org/10.1051/0004-6361/202038698

Millon M, Courbin F, Bonvin V, Paic E, Meylan G, Tewes M, Sluse D, Magain P, Chan JHH, Galan A, Joseph R, Lemon C, Tihhonova O, Anderson RI, Marmier M, Chazelas B, Lendl M, Triaud AHMJ, Wyttenbach A (2020a) COSMOGRAIL. XIX. Time delays in 18 strongly lensed quasars from 15 years of optical monitoring. Astron Astrophys 640:105. https://doi.org/10.1051/0004-6361/202037740

Millon M, Tewes M, Bonvin V, Lengen B, Courbin F (2020c) PyCS3: a python toolbox for time-delay measurements in lensed quasars. J Open Sour Softw 5(53):2654. https://doi.org/10.21105/joss.02654

More A, Verma A, Marshall PJ, More S, Baeten E, Wilcox J, Macmillan C, Cornen C, Kapadia A, Parrish M, Snyder C, Davis CP, Gavazzi R, Lintott CJ, Simpson R, Miller D, Smith AM, Paget E, Saha P, Küng R, Collett TE (2016) SPACE WARPS- II. New gravitational lens candidates from the CFHTLS discovered through citizen science. Mon Not R Astron Soc 455(2):1191–1210. https://doi.org/10.1093/mnras/stv1965

More A, Suyu SH, Oguri M, More S, Lee C-H (2017) Interpreting the strongly lensed supernova iPTF16geu: time delay predictions, microlensing, and lensing rates. Astrophys J Lett 835(2):25. https://doi.org/10.3847/2041-8213/835/2/L25

Mortonson MJ, Schechter PL, Wambsganss J (2005) Size is everything: universal features of quasar microlensing with extended sources. Astrophys J 628(2):594–603. https://doi.org/10.1086/431195

Mörtsell E, Johansson J, Dhawan S, Goobar A, Amanullah R, Goldstein DA (2020) Lens modelling of the strongly lensed type Ia supernova iPTF16geu. Mon Not R Astron Soc 496(3):3270–3280. https://doi.org/10.1093/mnras/staa1600

Narayan G, Zaidi T, Soraisam MD, Wang Z, Lochner M, Matheson T, Saha A, Yang S, Zhao Z, Kececioglu J, Scheidegger C, Snodgrass RT, Axelrod T, Jenness T, Maier RS, Ridgway ST, Seaman RL, Evans EM, Singh N, Taylor C, Toeniskoetter J, Welch E, Zhu S, ANTARES Collaboration (2018) Machine-learning-based brokers for real-time classification of the LSST alert stream. Astrophys J Suppl Ser 236(1):9. https://doi.org/10.3847/1538-4365/aab781

Newman AB, Belli S, Ellis RS, Patel SG (2018) Resolving quiescent galaxies at $z \gtrsim 2$. I. Search for gravitationally lensed sources and characterization of their structure, stellar populations, and line emission. Astrophys J 862(2):125. https://doi.org/10.3847/1538-4357/aacd4d

Noebauer UM, Kromer M, Taubenberger S, Baklanov P, Blinnikov S, Sorokina E, Hillebrandt W (2017) Early light curves for type Ia supernova explosion models. Mon Not R Astron Soc 472(3):2787–2799. https://doi.org/10.1093/mnras/stx2093

Nordin J, Brinnel V, van Santen J, Bulla M, Feindt U, Franckowiak A, Fremling C, Gal-Yam A, Giomi M, Kowalski M, Mahabal A, Miranda N, Rauch L, Reusch S, Rigault M, Schulze S, Sollerman J, Stein R,

Yaron O, van Velzen S, Ward C (2019) Transient processing and analysis using AMPEL: alert management, photometry, and evaluation of light curves. Astron Astrophys 631:147. https://doi.org/10.1051/0004-6361/201935634

Nugent P, Sullivan M, Ellis R, Gal-Yam A, Leonard DC, Howell DA, Astier P, Carlberg RG, Conley A, Fabbro S, Fouchez D, Neill JD, Pain R, Perrett K, Pritchet CJ, Regnault N (2006) Toward a cosmological Hubble diagram for type II-P supernovae. Astrophys J 645(2):841–850. https://doi.org/10.1086/504413

Nugent PE, Sullivan M, Cenko SB, Thomas RC, Kasen D, Howell DA, Bersier D, Bloom JS, Kulkarni SR, Kandrashoff MT, Filippenko AV, Silverman JM, Marcy GW, Howard AW, Isaacson HT, Maguire K, Suzuki N, Tarlton JE, Pan Y-C, Bildsten L, Fulton BJ, Parrent JT, Sand D, Podsiadlowski P, Bianco FB, Dilday B, Graham ML, Lyman J, James P, Kasliwal MM, Law NM, Quimby RM, Hook IM, Walker ES, Mazzali P, Pian E, Ofek EO, Gal-Yam A, Poznanski D (2011) Supernova SN 2011fe from an exploding carbon-oxygen white dwarf star. Nature 480(7377):344–347. https://doi.org/10.1038/nature10644

Oguri M (2019) Strong gravitational lensing of explosive transients. Rep Prog Phys 82(12):126901. https://doi.org/10.1088/1361-6633/ab4fc5

Oguri M, Marshall PJ (2010) Gravitationally lensed quasars and supernovae in future wide-field optical imaging surveys. Mon Not R Astron Soc 405(4):2579–2593. https://doi.org/10.1111/j.1365-2966.2010.16639.x

Østman L, Goobar A, Mörtsell E (2008) Extinction properties of lensing galaxies. Astron Astrophys 485(2):403–415. https://doi.org/10.1051/0004-6361:20079187

Paraficz D, Hjorth J (2009) Gravitational lenses as cosmic rulers: $\Omega_m$, $\Omega_\Lambda$ from time delays and velocity dispersions. Astron Astrophys 507(3):49–52. https://doi.org/10.1051/0004-6361/200913307

Pascale M, Frye BL, Dai L, Foo N, Qin Y, Leimbach R, Bauer AM, Merlin E, Coe D, Diego J, Yan H, Zitrin A, Cohen SH, Conselice CJ, Dole H, Harrington K, Jansen RA, Kamieneski P, Windhorst RA, Yun MS (2022) Possible ongoing merger discovered by photometry and spectroscopy in the field of the galaxy cluster PLCK G1657+67 0. Astrophys J 932(2):85. https://doi.org/10.3847/1538-4357/ac6ce9

Perlmutter S, Aldering G, Goldhaber G, Knop RA, Nugent P, Castro PG, Deustua S, Fabbro S, Goobar A, Groom DE, Hook IM, Kim AG, Kim MY, Lee JC, Nunes NJ, Pain R, Pennypacker CR, Quimby R, Lidman C, Ellis RS, Irwin M, McMahon RG, Ruiz-Lapuente P, Walton N, Schaefer B, Boyle BJ, Filippenko AV, Matheson T, Fruchter AS, Panagia N, Newberg HJM, Couch WJ, Project TSC (1999) Measurements of Ω and Λ from 42 high-redshift supernovae. Astrophys J 517(2):565–586. https://doi.org/10.1086/307221

Petrillo CE, Tortora C, Vernardos G, Koopmans LVE, Verdoes Kleijn G, Bilicki M, Napolitano NR, Chatterjee S, Covone G, Dvornik A, Erben T, Getman F, Giblin B, Heymans C, de Jong JTA, Kuijken K, Schneider P, Shan H, Spiniello C, Wright AH (2019) LinKS: discovering galaxy-scale strong lenses in the kilo-degree survey using convolutional neural networks. Mon Not R Astron Soc 484(3):3879–3896. https://doi.org/10.1093/mnras/stz189

Petrushevska T, Amanullah R, Goobar A, Fabbro S, Johansson J, Kjellsson T, Lidman C, Paech K, Richard J, Dahle H, Ferretti R, Kneib JP, Limousin M, Nordin J, Stanishev V (2016) High-redshift supernova rates measured with the gravitational telescope A 1689. Astron Astrophys 594:54. https://doi.org/10.1051/0004-6361/201628925

Petrushevska T, Amanullah R, Bulla M, Kromer M, Ferretti R, Goobar A, Papadogiannakis S (2017) Testing for redshift evolution of type Ia supernovae using the strongly lensed PS1-10afx at z = 1.4. Astron Astrophys 603:136. https://doi.org/10.1051/0004-6361/201730989

Pierel JDR, Rodney S (2019) Turning gravitationally lensed supernovae into cosmological probes. Astrophys J 876(2):107. https://doi.org/10.3847/1538-4357/ab164a

Pierel JDR, Rodney S, Vernardos G, Oguri M, Kessler R, Anguita T (2021) Projected cosmological constraints from strongly lensed supernovae with the roman space telescope. Astrophys J 908(2):190. https://doi.org/10.3847/1538-4357/abd8d3

Pierel JDR, Arendse N, Ertl S, Huang X, Moustakas LA, Schuldt S, Shajib AJ, Shu Y, Birrer S, Bronikowski M, Hjorth J, Suyu SH, Agarwal S, Agnello A, Bolton AS, Chakrabarti S, Cold C, Courbin F, Della Costa JM, Dhawan S, Engesser M, Fox OD, Gall C, Gomez S, Goobar A, Jimenez C, Johansson J, Li G, Marques-Chaves R, Mao S, Mazzali PA, Perez-Fournon I, Petrushevska T, Poidevin F, Rest A, Sheu W, Shirley R, Silver E, Storfer C, Treu T, Wojtak R, Zenati Y (2023) LensWatch: I. Resolved HST Observations and Constraints on the Strongly-Lensed Type Ia Supernova 2022qmx ("SN Zwicky"). Astrophys J 948:115. https://doi.org/10.3847/1538-4357/acc7a6. arXiv:2211.03772

Piro AL, Morozova VS (2016) Exploring the potential diversity of early type ia supernova light curves. Astrophys J 826(1):96. https://doi.org/10.3847/0004-637X/826/1/96

Piro AL, Nakar E (2014) Constraints on shallow $^{56}$Ni from the early light curves of type Ia supernovae. Astrophys J 784(1):85. https://doi.org/10.1088/0004-637X/784/1/85

Piro AL, Chang P, Weinberg NN (2010) Shock breakout from type Ia supernova. Astrophys J 708(1):598–604. https://doi.org/10.1088/0004-637X/708/1/598

Planck Collaboration, Aghanim N, Altieri B, Arnaud M, Ashdown M, Aumont J, Baccigalupi C, Banday AJ, Barreiro RB, Bartolo N, Battaner E, Beelen A, Benabed K, Benoit-Lévy A, Bernard J-P, Bersanelli M, Bethermin M, Bielewicz P, Bonavera L, Bond JR, Borrill J, Bouchet FR, Boulanger F, Burigana C, Calabrese E, Canameras R, Cardoso J-F, Catalano A, Chamballu A, Chary R-R, Chiang HC, Christensen PR, Clements DL, Colombi S, Couchot F, Crill BP, Curto A, Danese L, Dassas K, Davies RD, Davis RJ, de Bernardis P, de Rosa A, de Zotti G, Delabrouille J, Diego JM, Dole H, Donzelli S, Doré O, Douspis M, Ducout A, Dupac X, Efstathiou G, Elsner F, Enßlin TA, Falgarone E, Flores-Cacho I, Forni O, Frailis M, Fraisse AA, Franceschi E, Frejsel A, Frye B, Galeotta S, Galli S, Ganga K, Giard M, Gjerløw E, González-Nuevo J, Górski KM, Gregorio A, Gruppuso A, Guéry D, Hansen FK, Hanson D, Harrison DL, Helou G, Hernández-Monteagudo C, Hildebrandt SR, Hivon E, Hobson M, Holmes WA, Hovest W, Huffenberger KM, Hurier G, Jaffe AH, Jaffe TR, Keihänen E, Keskitalo R, Kisner TS, Kneissl R, Knoche J, Kunz M, Kurki-Suonio H, Lagache G, Lamarre J-M, Lasenby A, Lattanzi M, Lawrence CR, Le Floc'h E, Leonardi R, Levrier F, Liguori M, Lilje PB, Linden-Vørnle M, López-Caniego M, Lubin PM, Macías-Pérez JF, MacKenzie T, Maffei B, Mandolesi N, Maris M, Martin PG, Martinache C, Martí nez-González E, Masi S, Matarrese S, Mazzotta P, Melchiorri A, Mennella A, Migliaccio M, Moneti A, Montier L, Morgante G, Mortlock D, Munshi D, Murphy JA, Natoli P, Negrello M, Nesvadba NPH, Novikov D, Novikov I, Omont A, Pagano L, Pajot F, Pasian F, Perdereau O, Perotto L, Perrotta F, Pettorino V, Piacentini F, Piat M, Plaszczynski S, Pointecouteau E, Polenta G, Popa L, Pratt GW, Prunet S, Puget J-L, Rachen JP, Reach WT, Reinecke M, Remazeilles M, Renault C, Ristorcelli I, Rocha G, Roudier G, Rusholme B, Sandri M, Santos D, Savini G, Scott D, Spencer LD, Stolyarov V, Sunyaev R, Sutton D, Sygnet J-F, Tauber JA, Terenzi L, Toffolatti L, Tomasi M, Tristram M, Tucci M, Umana G, Valenziano L, Valiviita J, Valtchanov I, Van Tent B, Vieira JD, Vielva P, Wade LA, Wandelt BD, Wehus IK, Welikala N, Zacchei A, Zonca A (2015) Planck intermediate results. XXVII. High-redshift infrared galaxy overdensity candidates and lensed sources discovered by Planck and confirmed by Herschel-SPIRE. Astron Astrophys 582:30. https://doi.org/10.1051/0004-6361/201424790

Planck Collaboration, Aghanim N, Akrami Y, Ashdown M, Aumont J, Baccigalupi C, Ballardini M, Banday AJ, Barreiro RB, Bartolo N, Basak S, Battye R, Benabed K, Bernard J-P, Bersanelli M, Bielewicz P, Bock JJ, Bond JR, Borrill J, Bouchet FR, Boulanger F, Bucher M, Burigana C, Butler RC, Calabrese E, Cardoso J-F, Carron J, Challinor A, Chiang HC, Chluba J, Colombo LPL, Combet C, Contreras D, Crill BP, Cuttaia F, de Bernardis P, de Zotti G, Delabrouille J, Delouis J-M, Di Valentino E, Diego JM, Doré O, Douspis M, Ducout A, Dupac X, Dusini S, Efstathiou G, Elsner F, Enßlin TA, Eriksen HK, Fantaye Y, Farhang M, Fergusson J, Fernandez-Cobos R, Finelli F, Forastieri F, Frailis M, Fraisse AA, Franceschi E, Frolov A, Galeotta S, Galli S, Ganga K, Génova-Santos RT, Gerbino M, Ghosh T, González-Nuevo J, Górski KM, Gratton S, Gruppuso A, Gudmundsson JE, Hamann J, Handley W, Hansen FK, Herranz D, Hildebrandt SR, Hivon E, Huang Z, Jaffe AH, Jones WC, Karakci A, Keihänen E, Keskitalo R, Kiiveri K, Kim J, Kisner TS, Knox L, Krachmalnicoff N, Kunz M, Kurki-Suonio H, Lagache G, Lamarre J-M, Lasenby A, Lattanzi M, Lawrence CR, Le Jeune M, Lemos P, Lesgourgues J, Levrier F, Lewis A, Liguori M, Lilje PB, Lilley M, Lindholm V, López-Caniego M, Lubin PM, Ma Y-Z, Macías-Pérez JF, Maggio G, Maino D, Mandolesi N, Mangilli A, Marcos-Caballero A, Maris M, Martin PG, Martinelli M, Martí nez-González E, Matarrese S, Mauri N, McEwen JD, Meinhold PR, Melchiorri A, Mennella A, Migliaccio M, Millea M, Mitra S, Miville-Deschênes M-A, Molinari D, Montier L, Morgante G, Moss A, Natoli P, Nørgaard-Nielsen HU, Pagano L, Paoletti D, Partridge B, Patanchon G, Peiris HV, Perrotta F, Pettorino V, Piacentini F, Polastri L, Polenta G, Puget J-L, Rachen JP, Reinecke M, Remazeilles M, Renzi A, Rocha G, Rosset C, Roudier G, Rubiño-Martí n JA, Ruiz-Granados B, Salvati L, Sandri M, Savelainen M, Scott D, Shellard EPS, Sirignano C, Sirri G, Spencer LD, Sunyaev R, Suur-Uski A-S, Tauber JA, Tavagnacco D, Tenti M, Toffolatti L, Tomasi M, Trombetti T, Valenziano L, Valiviita J, Van Tent B, Vibert L, Vielva P, Villa F, Vittorio N, Wandelt BD, Wehus IK, White M, White SDM, Zacchei A, Zonca A (2020) Planck 2018 results. VI. Cosmological parameters. Astron Astrophys 641:6. https://doi.org/10.1051/0004-6361/201833910

Polletta M, Nonino M, Frye B, Gargiulo A, Bisogni S, Garuda N, Thompson D, Lehnert M, Pascale M, Willner SP, Kamieneski P, Leimbach R, Cheng C, Coe D, Cohen SH, Conselice CJ, Dai L, Diego J, Dole H, Driver SP, D'Silva JCJ, Fontana A, Foo N, Furtak LJ, Grogin NA, Harrington K, Hathi NP, Jansen RA, Kelly P, Koekemoer AM, Mancini C, Marshall MA, Pierel JDR, Pirzkal N, Robotham A, Rutkowski MJ, Ryan RE, Snigula JM, Summers J, Tompkins S, Willmer CNA, Windhorst RA, Yan H, Yun MS, Zitrin A (2023) Spectroscopy of the supernova H0pe host galaxy at redshift 1.78. Astron Astrophys 675:4. https://doi.org/10.1051/0004-6361/202346964

Quimby RM, Werner MC, Oguri M, More S, More A, Tanaka M, Nomoto K, Moriya TJ, Folatelli G, Maeda K, Bersten M (2013) Extraordinary magnification of the ordinary type Ia supernova PS1-10afx. Astrophys J Lett 768(1):20. https://doi.org/10.1088/2041-8205/768/1/L20

Quimby RM, Oguri M, More A, More S, Moriya TJ, Werner MC, Tanaka M, Folatelli G, Bersten MC, Maeda K, Nomoto K (2014) Detection of the gravitational lens magnifying a type Ia supernova. Science 344(6182):396–399. https://doi.org/10.1126/science.1250903

Rabinak I, Waxman E (2011) The early UV/optical emission from core-collapse supernovae. Astrophys J 728(1):63. https://doi.org/10.1088/0004-637X/728/1/63

Refsdal S (1964) On the possibility of determining Hubble's parameter and the masses of galaxies from the gravitational lens effect. Mon Not R Astron Soc 128:307. https://doi.org/10.1093/mnras/128.4.307

Riess AG, Filippenko AV, Challis P, Clocchiatti A, Diercks A, Garnavich PM, Gilliland RL, Hogan CJ, Jha S, Kirshner RP, Leibundgut B, Phillips MM, Reiss D, Schmidt BP, Schommer RA, Smith RC, Spyromilio J, Stubbs C, Suntzeff NB, Tonry J (1998) Observational evidence from supernovae for an accelerating universe and a cosmological constant. Astron J 116(3):1009–1038. https://doi.org/10.1086/300499

Riess AG, Casertano S, Yuan W, Macri LM, Scolnic D (2019) Large Magellanic Cloud Cepheid standards provide a 1% foundation for the determination of the Hubble constant and stronger evidence for physics beyond ΛCDM. Astrophys J 876(1):85. https://doi.org/10.3847/1538-4357/ab1422

Rodney SA, Riess AG, Dahlen T, Strolger L-G, Ferguson HC, Hjorth J, Frederiksen TF, Weiner BJ, Mobasher B, Casertano S, Jones DO, Challis P, Faber SM, Filippenko AV, Garnavich P, Graur O, Grogin NA, Hayden B, Jha SW, Kirshner RP, Kocevski D, Koekemoer A, McCully C, Patel B, Rajan A, Scarlata C (2012) A type Ia supernova at redshift 1.55 in Hubble Space Telescope infrared observations from CANDELS. Astrophys J 746(1):5. https://doi.org/10.1088/0004-637X/746/1/5

Rodney SA, Strolger L-G, Kelly PL, Bradač M, Brammer G, Filippenko AV, Foley RJ, Graur O, Hjorth J, Jha SW, McCully C, Molino A, Riess AG, Schmidt KB, Selsing J, Sharon K, Treu T, Weiner BJ, Zitrin A (2016) SN refsdal: photometry and time delay measurements of the first Einstein cross supernova. Astrophys J 820(1):50. https://doi.org/10.3847/0004-637X/820/1/50

Rodney SA, Brammer GB, Pierel JDR, Richard J, Toft S, O'Connor KF, Akhshik M, Whitaker K (2021) A gravitationally lensed supernova with an observable two-decade time delay. Nat Astron 5:1118. https://doi.org/10.1038/s41550-021-01450-9. arXiv:2106.08935

Rojas K, Savary E, Clément B, Maus M, Courbin F, Lemon C, Chan JHH, Vernardos G, Joseph R, Cañameras R, Galan A (2022) Search of strong lens systems in the dark energy survey using convolutional neural networks. Astron Astrophys 668:73. https://doi.org/10.1051/0004-6361/202142119

Röpke FK, Kromer M, Seitenzahl IR, Pakmor R, Sim SA, Taubenberger S, Ciaraldi-Schoolmann F, Hillebrandt W, Aldering G, Antilogus P, Baltay C, Benitez-Herrera S, Bongard S, Buton C, Canto A, Cellier-Holzem F, Childress M, Chotard N, Copin Y, Fakhouri HK, Fink M, Fouchez D, Gangler E, Guy J, Hachinger S, Hsiao EY, Chen J, Kerschhaggl M, Kowalski M, Nugent P, Paech K, Pain R, Pecontal E, Pereira R, Perlmutter S, Rabinowitz D, Rigault M, Runge K, Saunders C, Smadja G, Suzuki N, Tao C, Thomas RC, Tilquin A, Wu C (2012) Constraining type Ia supernova models: SN 2011fe as a test case. Astrophys J Lett 750(1):19. https://doi.org/10.1088/2041-8205/750/1/L19

Saha A, Matheson T, Snodgrass R, Kececioglu J, Narayan G, Seaman R, Jenness T, Axelrod T (2014) ANTARES: a prototype transient broker system. In: Peck AB, Benn CR, Seaman RL (eds) Observatory operations: strategies, processes, and systems V. Society of photo-optical instrumentation engineers (SPIE) conference series, vol 9149, p 914908. https://doi.org/10.1117/12.2056988

Savary E, Rojas K, Maus M, Clément B, Courbin F, Gavazzi R, Chan JHH, Lemon C, Vernardos G, Cañameras R, Schuldt S, Suyu SH, Cuillandre J-C, Fabbro S, Gwyn S, Hudson MJ, Kilbinger M, Scott D, Stone C (2022) Strong lensing in UNIONS: toward a pipeline from discovery to modeling. Astron Astrophys 666:1. https://doi.org/10.1051/0004-6361/202142505

Schechter PL, Wambsganss J (2002) Quasar microlensing at high magnification and the role of dark matter: enhanced fluctuations and suppressed saddle points. Astrophys J 580(2):685–695. https://doi.org/10.1086/343856

Schlafly EF, Meisner AM, Stutz AM, Kainulainen J, Peek JEG, Tchernyshyov K, Rix H-W, Finkbeiner DP, Covey KR, Green GM, Bell EF, Burgett WS, Chambers KC, Draper PW, Flewelling H, Hodapp KW, Kaiser N, Magnier EA, Martin NF, Metcalfe N, Wainscoat RJ, Waters C (2016) The optical-infrared extinction curve and its variation in the Milky Way. Astrophys J 821(2):78. https://doi.org/10.3847/0004-637X/821/2/78

Schlafly EF, Peek JEG, Finkbeiner DP, Green GM (2017) Mapping the extinction curve in 3d: structure on kiloparsec scales. Astrophys J 838(1):36. https://doi.org/10.3847/1538-4357/aa619d

Schneider P (2014) Can one determine cosmological parameters from multi-plane strong lens systems? Astron Astrophys 568:2. https://doi.org/10.1051/0004-6361/201424450

Schneider P, Sluse D (2014) Source-position transformation: an approximate invariance in strong gravitational lensing. Astron Astrophys 564:103. https://doi.org/10.1051/0004-6361/201322106

Scolnic DM, Jones DO, Rest A, Pan YC, Chornock R, Foley RJ, Huber ME, Kessler R, Narayan G, Riess AG, Rodney S, Berger E, Brout DJ, Challis PJ, Drout M, Finkbeiner D, Lunnan R, Kirshner RP, Sanders NE, Schlafly E, Smartt S, Stubbs CW, Tonry J, Wood-Vasey WM, Foley M, Hand J, Johnson E, Burgett WS,

Chambers KC, Draper PW, Hodapp KW, Kaiser N, Kudritzki RP, Magnier EA, Metcalfe N, Bresolin F, Gall E, Kotak R, McCrum M, Smith KW (2018) The complete light-curve sample of spectroscopically confirmed SNe ia from pan-STARRS1 and cosmological constraints from the combined pantheon sample. Astrophys J 859(2):101. https://doi.org/10.3847/1538-4357/aab9bb

Shajib AJ, Birrer S, Treu T, Auger MW, Agnello A, Anguita T, Buckley-Geer EJ, Chan JHH, Collett TE, Courbin F, Fassnacht CD, Frieman J, Kayo I, Lemon C, Lin H, Marshall PJ, McMahon R, More A, Morgan ND, Motta V, Oguri M, Ostrovski F, Rusu CE, Schechter PL, Shanks T, Suyu SH, Meylan G, Abbott TMC, Allam S, Annis J, Avila S, Bertin E, Brooks D, Carnero Rosell A, Carrasco Kind M, Carretero J, Cunha CE, da Costa LN, De Vicente J, Desai S, Doel P, Flaugher B, Fosalba P, García-Bellido J, Gerdes DW, Gruen D, Gruendl RA, Gutierrez G, Hartley WG, Hollowood DL, Hoyle B, James DJ, Kuehn K, Kuropatkin N, Lahav O, Lima M, Maia MAG, March M, Marshall JL, Melchior P, Menanteau F, Miquel R, Plazas AA, Sanchez E, Scarpine V, Sevilla-Noarbe I, Smith M, Soares-Santos M, Sobreira F, Suchyta E, Swanson MEC, Tarle G, Walker AR (2019) Is every strong lens model unhappy in its own way? Uniform modelling of a sample of 13 quadruply+ imaged quasars. Mon Not R Astron Soc 483(4):5649–5671. https://doi.org/10.1093/mnras/sty3397

Shajib AJ, Mozumdar P, Chen GC-F, Treu T, Cappellari M, Knabel S, Suyu SH, Bennert VN, Frieman JA, Sluse D, Birrer S, Courbin F, Fassnacht CD, Villafaña L, Williams PR (2023) TDCOSMO. XIII. Improved Hubble constant measurement from lensing time delays using spatially resolved stellar kinematics of the lens galaxy. Astron Astrophys 673:A9. https://doi.org/10.1051/0004-6361/202345878. arXiv:2301.02656

Sherstinsky A (2020) Fundamentals of recurrent neural network (RNN) and long short-term memory (LSTM) network. Phys D: Nonlinear Phenom 404:132306. https://doi.org/10.1016/j.physd.2019.132306

Sheu W, Huang X, Cikota A, Suzuki N, Schlegel D, Storfer C (2023) Retrospective search for strongly lensed supernovae in the DESI Legacy Imaging Surveys. Astrophys J 952(1):10. https://doi.org/10.3847/1538-4357/acd1e4. arXiv:2301.03578

Shu Y, Brownstein JR, Bolton AS, Koopmans LVE, Treu T, Montero-Dorta AD, Auger MW, Czoske O, Gavazzi R, Marshall PJ, Moustakas LA (2017) The sloan lens ACS survey. XIII. Discovery of 40 new galaxy-scale strong lenses. Astrophys J 851(1):48. https://doi.org/10.3847/1538-4357/aa9794

Shu Y, Bolton AS, Mao S, Kang X, Li G, Soraisam M (2018a) Prediction of supernova rates in known galaxy-galaxy strong-lens systems. Astrophys J 864(1):91. https://doi.org/10.3847/1538-4357/aad5ea

Shu Y, Bolton AS, Mao S, Kang X, Li G, Soraisam M (2021) Erratum: "Prediction of supernova rates in known galaxy-galaxy strong-lens systems" (2018, ApJ, 864, 91). Astrophys J 919(1):67. https://doi.org/10.3847/1538-4357/ac24a4

Shu Y, Cañameras R, Schuldt S, Suyu SH, Taubenberger S, Inoue KT, Jaelani AT, High-redshift HOLISMOKESVIII (2022) Strong-lens search in the hyper suprime-cam subaru strategic program. Astron Astrophys 662:4. https://doi.org/10.1051/0004-6361/202243203

Sim SA, Röpke FK, Hillebrandt W, Kromer M, Pakmor R, Fink M, Ruiter AJ, Seitenzahl IR (2010) Detonations in sub-Chandrasekhar-mass C+O white dwarfs. Astrophys J Lett 714(1):52–57. https://doi.org/10.1088/2041-8205/714/1/L52

Smith KW, Williams RD, Young DR, Ibsen A, Smartt SJ, Lawrence A, Morris D, Voutsinas S, Nicholl M (2019) Lasair: the transient alert broker for LSST:UK. Res. Notes Am. Astron. Soc. 3(1):26. https://doi.org/10.3847/2515-5172/ab020f

Sonnenfeld A, Chan JHH, Shu Y, More A, Oguri M, Suyu SH, Wong KC, Lee C-H, Coupon J, Yonehara A, Bolton AS, Jaelani AT, Tanaka M, Miyazaki S, Komiyama Y (2018) Survey of gravitationally-lensed objects in HSC imaging (SuGOHI). I. Automatic search for galaxy-scale strong lenses. Publ Astron Soc Jpn 70:29. https://doi.org/10.1093/pasj/psx062

Sonnenfeld A, Verma A, More A, Baeten E, Macmillan C, Wong KC, Chan JHH, Jaelani AT, Lee C-H, Oguri M, Rusu CE, Veldthuis M, Trouille L, Marshall PJ, Hutchings R, Allen C, O'Donnell J, Cornen C, Davis CP, McMaster A, Lintott C, Miller G (2020) Survey of gravitationally-lensed objects in HSC imaging (SuGOHI). VI. Crowdsourced lens finding with space warps. Astron Astrophys 642:148. https://doi.org/10.1051/0004-6361/202038067

Stanishev V, Goobar A, Paech K, Amanullah R, Dahlén T, Jönsson J, Kneib JP, Lidman C, Limousin M, Mörtsell E, Nobili S, Richard J, Riehm T, von Strauss M (2009) Near-IR search for lensed supernovae behind galaxy clusters. I. Observations and transient detection efficiency. Astron Astrophys 507(1):61–69. https://doi.org/10.1051/0004-6361/200911982

Sullivan M, Ellis R, Nugent P, Smail I, Madau P (2000) A strategy for finding gravitationally lensed distant supernovae. Mon Not R Astron Soc 319(2):549–556. https://doi.org/10.1046/j.1365-8711.2000.03875.x

Suwa Y (2018) Supernova forecast with strong lensing. Mon Not R Astron Soc 474(2):2612–2616. https://doi.org/10.1093/mnras/stx2953

Suyu SH, Marshall PJ, Auger MW, Hilbert S, Blandford RD, Koopmans LVE, Fassnacht CD, Treu T (2010) Dissecting the gravitational lens B1608+656. II. Precision measurements of the Hubble constant, spatial

curvature, and the dark energy equation of state. Astrophys J 711(1):201–221. https://doi.org/10.1088/0004-637X/711/1/201

Suyu SH, Chang T-C, Courbin F, Okumura T (2018) Cosmological distance indicators. Space Sci Rev 214(5):91. https://doi.org/10.1007/s11214-018-0524-3

Suyu SH, Huber S, Cañameras R, Kromer M, Schuldt S, Taubenberger S, Yıldırım A, Bonvin V, Chan JHH, Courbin F, Nöbauer U, Sim SA, Sluse D (2020) HOLISMOKES. I. Highly optimised lensing investigations of supernovae, microlensing objects, and kinematics of ellipticals and spirals. Astron Astrophys 644:162. https://doi.org/10.1051/0004-6361/202037757

Tewes M, Courbin F, Meylan G (2013) COSMOGRAIL: the COSmological MOnitoring of GRAvItational lenses. XI. Techniques for time delay measurement in presence of microlensing. Astron Astrophys 553:120. https://doi.org/10.1051/0004-6361/201220123

Tran K-VH, Harshan A, Glazebrook K, Keerthi Vasan GC, Jones T, Jacobs C, Kacprzak GG, Barone TM, Collett TE, Gupta A, Henderson A, Kewley LJ, Lopez S, Nanayakkara T, Sanders RL, Sweet SM (2022) The AGEL survey: spectroscopic confirmation of strong gravitational lenses in the DES and DECaLS fields selected using convolutional neural networks. Astron J 164(4):148. https://doi.org/10.3847/1538-3881/ac7da2

Treu T, Marshall PJ (2016) Time delay cosmography. Astron Astrophys Rev 24(1):11. https://doi.org/10.1007/s00159-016-0096-8

Treu T, Brammer G, Diego JM, Grillo C, Kelly PL, Oguri M, Rodney SA, Rosati P, Sharon K, Zitrin A, Balestra I, Bradač M, Broadhurst T, Caminha GB, Halkola A, Hoag A, Ishigaki M, Johnson TL, Karman W, Kawamata R, Mercurio A, Schmidt KB, Strolger L-G, Suyu SH, Filippenko AV, Foley RJ, Jha SW, Patel B (2016) "Refsdal" meets popper: comparing predictions of the re-appearance of the multiply imaged supernova behind MACSJ1149.5+2223. Astrophys J 817(1):60. https://doi.org/10.3847/0004-637X/817/1/60

Treu T, Suyu SH, Marshall PJ (2022) Strong lensing time-delay cosmography in the 2020s. Astron Astrophys Rev 30(1):8. https://doi.org/10.1007/s00159-022-00145-y

Verde L, Treu T, Riess AG (2019) Tensions between the early and late universe. Nat Astron 3:891–895. https://doi.org/10.1038/s41550-019-0902-0

Vernardos G, Fluke CJ (2014) Adventures in the microlensing cloud: large datasets, eResearch tools, and GPUs. Astron Comput 6:1–18. https://doi.org/10.1016/j.ascom.2014.05.002

Vernardos G, Tsagkatakis G (2019) Quasar microlensing light-curve analysis using deep machine learning. Mon Not R Astron Soc 486(2):1944–1952. https://doi.org/10.1093/mnras/stz868

Vernardos G, Fluke CJ, Bate NF, Croton D (2014) GERLUMPH data release 1: high-resolution cosmological microlensing magnification maps and eResearch tools. Astrophys J Suppl Ser 211(1):16. https://doi.org/10.1088/0067-0049/211/1/16

Vernardos G, Fluke CJ, Bate NF, Croton D, Vohl D (2015) GERLUMPH data release 2: 2.5 billion simulated microlensing light curves. Astrophys J Suppl Ser 217(2):23. https://doi.org/10.1088/0067-0049/217/2/23

Vernardos G et al (2023) Microlensing of strongly lensed quasars. arXiv:2312.00931

Vieira JD, Marrone DP, Chapman SC, De Breuck C, Hezaveh YD, Weiß A, Aguirre JE, Aird KA, Aravena M, Ashby MLN, Bayliss M, Benson BA, Biggs AD, Bleem LE, Bock JJ, Bothwell M, Bradford CM, Brodwin M, Carlstrom JE, Chang CL, Crawford TM, Crites AT, de Haan T, Dobbs MA, Fomalont EB, Fassnacht CD, George EM, Gladders MD, Gonzalez AH, Greve TR, Gullberg B, Halverson NW, High FW, Holder GP, Holzapfel WL, Hoover S, Hrubes JD, Hunter TR, Keisler R, Lee AT, Leitch EM, Lueker M, Luong-van D, Malkan M, McIntyre V, McMahon JJ, Mehl J, Menten KM, Meyer SS, Mocanu LM, Murphy EJ, Natoli T, Padin S, Plagge T, Reichardt CL, Rest A, Ruel J, Ruhl JE, Sharon K, Schaffer KK, Shaw L, Shirokoff E, Spilker JS, Stalder B, Staniszewski Z, Stark AA, Story K, Vanderlinde K, Welikala N, Williamson R (2013) Dusty starburst galaxies in the early universe as revealed by gravitational lensing. Nature 495(7441):344–347. https://doi.org/10.1038/nature12001

Vogl C, Sim SA, Noebauer UM, Kerzendorf WE, Hillebrandt W (2019) Spectral modeling of type II supernovae. I. Dilution factors. Astron Astrophys 621:29. https://doi.org/10.1051/0004-6361/201833701

Vogl C, Kerzendorf WE, Sim SA, Noebauer UM, Lietzau S, Hillebrandt W (2020) Spectral modeling of type II supernovae. II. A machine-learning approach to quantitative spectroscopic analysis. Astron Astrophys 633:88. https://doi.org/10.1051/0004-6361/201936137

Walsh D, Carswell RF, Weymann RJ (1979) 0957+561 A, B: twin quasistellar objects or gravitational lens? Nature 279:381–384. https://doi.org/10.1038/279381a0

Webbink RF (1984) Double white dwarfs as progenitors of R coronae borealis stars and type I supernovae. Astrophys J 277:355–360. https://doi.org/10.1086/161701

Weisenbach L, Schechter PL, Pontula S (2021) "Worst-case" microlensing in the identification and modeling of lensed quasars. Astrophys J 922(1):70. https://doi.org/10.3847/1538-4357/ac2228

Whelan J, Iben I Jr (1973) Binaries and supernovae of type I. Astrophys J 186:1007–1014. https://doi.org/10.1086/152565

Wojtak R, Hjorth J, Gall C (2019) Magnified or multiply imaged? - search strategies for gravitationally lensed supernovae in wide-field surveys. Mon Not R Astron Soc 487(3):3342–3355. https://doi.org/10.1093/mnras/stz1516

Wong KC, Suyu SH, Chen GC-F, Rusu CE, Millon M, Sluse D, Bonvin V, Fassnacht CD, Taubenberger S, Auger MW, Birrer S, Chan JHH, Courbin F, Hilbert S, Tihhonova O, Treu T, Agnello A, Ding X, Jee I, Komatsu E, Shajib AJ, Sonnenfeld A, Blandford RD, Koopmans LVE, Marshall PJ, Meylan G (2020) H0LiCOW – XIII. A 2.4 per cent measurement of $H_0$ from lensed quasars: 5.3$\sigma$ tension between early- and late-Universe probes. Mon Not R Astron Soc 498(1):1420–1439. https://doi.org/10.1093/mnras/stz3094

Yahalomi DA, Schechter PL, Wambsganss J (2017) A Quadruply Lensed SN Ia: Gaining a Time-Delay...Losing a Standard Candle. ArXiv e-prints, arXiv:1711.07919

Yao Y, Miller AA, Kulkarni SR, Bulla M, Masci FJ, Goldstein DA, Goobar A, Nugent P, Dugas A, Blagorodnova N, Neill JD, Rigault M, Sollerman J, Nordin J, Bellm EC, Cenko SB, De K, Dhawan S, Feindt U, Fremling C, Gatkine P, Graham MJ, Graham ML, Ho AYQ, Hung T, Kasliwal MM, Kupfer T, Laher RR, Perley DA, Rusholme B, Shupe DL, Soumagnac MT, Taggart K, Walters R, Yan L (2019) ZTF early observations of type Ia supernovae. I. Properties of the 2018 sample. Astrophys J 886(2):152. https://doi.org/10.3847/1538-4357/ab4cf5

Yıldırım A, Suyu SH, Halkola A (2020) Time-delay cosmographic forecasts with strong lensing and JWST stellar kinematics. Mon Not R Astron Soc 493(4):4783–4807. https://doi.org/10.1093/mnras/staa498

Yıldırım A, Suyu SH, Chen GC-F, Komatsu E (2023) TDCOSMO VIII: Cosmological distance measurements in light of the mass-sheet degeneracydegeneracy: Forecasts from strong lensing and integral field unit stellar kinematics. Astron Astrophys 675:A21. https://doi.org/10.1051/0004-6361/202142318. arXiv:2109.14615

Zwicky F (1937) Nebulae as gravitational lenses. Phys Rev 51:290–290. https://doi.org/10.1103/PhysRev.51.290



## Authors and Affiliations

**Sherry H. Suyu[1,2,3] · Ariel Goobar[4] · Thomas Collett[5] · Anupreeta More[6,7] · Giorgos Vernardos[8]**

✉ S.H. Suyu
suyu@mpa-garching.mpg.de

A. Goobar
ariel@fysik.su.se

T. Collett
thomas.collett@port.ac.uk

A. More
anupreeta@iucaa.in

G. Vernardos
georgios.vernardos@epfl.ch

1 TUM School of Natural Sciences, Department of Physics, Technical University of Munich, James-Franck-Straße 1, 85748 Garching, Germany

2 Max-Planck-Institut für Astrophysik, Karl-Schwarzschild-Str. 1, 85748 Garching, Germany

3 Institute of Astronomy and Astrophysics, Academia Sinica, 11F of ASMAB, No.1, Sect. 4, Roosevelt Road, Taipei 10617, Taiwan

4 The Oskar Klein Centre, Department of Physics, Stockholm University, Albanova University Center, SE-106 91 Stockholm, Sweden

[5] Institute of Cosmology and Gravitation, University of Portsmouth, Dennis Sciama Building, Burnaby Road, Portsmouth, PO1 3FX, UK

[6] The Inter-University Centre for Astronomy and Astrophysics (IUCAA), Post Bag 4, Ganeshkhind, Pune 411007, India

[7] Kavli Institute for the Physics and Mathematics of the Universe (IPMU), 5-1-5 Kashiwanoha, Kashiwa-shi, Chiba 277-8583, Japan

[8] Institute of Physics, Laboratory of Astrophysics, Ecole Polytechnique Fédérale de Lausanne (EPFL), Observatoire de Sauverny, 1290 Versoix, Switzerland